

THE MACHO PROJECT LMC VARIABLE STAR INVENTORY. IX. FREQUENCY ANALYSIS OF THE FIRST OVERTONE RR LYRAE STARS AND THE INDICATION FOR NONRADIAL PULSATIONS

ALCOCK, C.¹, ALLSMAN, R.², ALVES, D. R.³, AXELROD, T.², BECKER, A.⁴, BENNETT, D.¹², CLEMENT, C.¹⁵, COOK, K.H.¹, DRAKE, A.², FREEMAN, K.², GEHA, M.¹, GRIEST, K.⁵, KOVÁCS, G.¹³, KURTZ, D.W.¹⁴, LEHNER, M.¹¹, MARSHALL, S.¹, MINNITI, D.⁶, NELSON, C.^{1,7}, PETERSON, B.², POPOWSKI, P.¹, PRATT, M.⁴, QUINN, P.⁸, RODGERS, A.¹⁶, ROWE, J.¹⁵, STUBBS, C.⁴, SUTHERLAND, W.⁹, TOMANEY, A.⁴, VANDEHEI, T.⁵ AND WELCH, D.L.¹⁰

Draft version November 25, 2018

ABSTRACT

More than 1300 variables classified provisionally as first overtone RR Lyrae pulsators in the MACHO variable star database of the Large Magellanic Cloud (LMC) have been subjected to standard frequency analysis. Based on the remnant power in the prewhitened spectra, we found 70% of the total population to be monop periodic. The remaining 30% (411 stars) are classified as one of 9 types according to their frequency spectra. Several types of RR Lyrae pulsational behavior are clearly identified here for the first time. Together with the earlier discovered double-mode (fundamental & first overtone) variables this study increased the number of the known double-mode stars in the LMC to 181. During the total 6.5 yr time span of the data, 10% of the stars show strong period changes. The size, and in general also the patterns of the period changes exclude simple evolutionary explanation. We also discovered two additional types of multifrequency pulsators with low occurrence rates of 2% for each. In the first type there remains one closely spaced component after prewhitening by the main pulsation frequency. In the second type the number of remnant components is two, they are also closely spaced, and, in addition, they are symmetric in their frequency spacing relative to the central component. This latter type of variables is associated with their relatives among the fundamental pulsators, known as Blazhko variables. Their high frequency ($\approx 20\%$) among the fundamental mode variables versus the low occurrence rate of their first overtone counterparts makes it more difficult to explain Blazhko phenomenon by any theory depending mainly on the role of aspect angle or magnetic field. None of the current theoretical models are able to explain the observed close frequency components without invoking nonradial pulsation components in these stars.

Subject headings: globular clusters: general — stars: horizontal-branch — stars: oscillations — stars: variables: other (RR Lyrae)

¹Institute for Geophysics and Planetary Physics, Lawrence Livermore National Laboratory, Livermore, CA 94550, USA
alcock, kcook, mgeha, stuart, cnelson, popowski1@llnl.gov

²Mount Stromlo and Siding Spring Observatory, Australian National University, Weston Creek, ACT 0200, Australia
ajd, kcf, peterson, tsa@mso.anu.edu.au, robyn@mindful.anu.edu.au

³Space Telescope Science Institute, Baltimore, MD 21218, USA
alves@stsci.edu

⁴Department of Astronomy, University of Washington, Seattle, WA 98195, USA
austin, becker, stubbs@astro.washington.edu

⁵Department of Physics, University of California, San Diego, CA 92093, USA
kgriest, tvandehai@ucsd.edu

⁶Department Astronomia, Universidad Catolica, Chile
dante@astro.puc.cl

⁷Department of Physics, University of California, Berkeley, CA 94720, USA

⁸European Southern Observatory, Garching, D-85748, Germany
pjq@eso.org

⁹Department of Physics, Oxford University, OX1 3RH, England
w.sutherland@physics.ox.ac.uk

¹⁰Department of Physics and Astronomy, McMaster University, Hamilton, L82 4M1, Canada
welch@physics.mcmaster.ca

¹¹Department of Physics, University of Sheffield, S3 7RH, England

¹²Department of Physics, University of Notre Dame, South Bend, IN 46556, USA
bennett@nd.edu

¹³Konkoly Observatory, P.O. Box 67, H-1525 Budapest, Hungary
kovacs@konkoly.hu

¹⁴Department of Astronomy, University of Cape Town, Rondebosch 7701, South Africa
dkurtz@ma.saa.ac.za

¹⁵Department of Astronomy, University of Toronto, Toronto, M5S 3H8, Canada
cclement, rowe@astro.utoronto.ca

¹⁶deceased

1. INTRODUCTION

In this continuing series of papers dealing with the variable star data of the MACHO project, we examine here the temporal behavior of a large sample of *first overtone RR Lyrae* stars. Until very recently, short-periodic RR Lyrae stars have been known to appear in two different flavors: (a) singly-periodic; (b) doubly-periodic (or double-mode). In this latter case the two periods are associated with the first two radial normal modes of the star. Because of their dominant first overtone content, these variables were hidden for a long period of time among the monophasic first overtone stars. In 1977 AQ Leo was discovered as the first double-mode RR Lyrae star by Jerzykiewicz & Wenzel (1977). The first variable of this type in a globular cluster was discovered by Goranskij (1981). However, it was only in 1983 when the first systematic studies started in globular clusters (Cox, Hodson & Clancy 1983), although there were suggestions that some of the first overtone variables in the appropriate period range with 'excessive scatter' might be actually double-mode stars (Sandage, Katem & Sandage 1981).

Less than a year ago Olech et al. (1999a, b, hereafter O99a,b) found that some first overtone stars in the globular clusters M5 and M55 exhibit two frequencies, very closely spaced. They argued that the high period ratio strongly indicated the presence of nonradial modes in those stars. In the course of another recent study of the pulsation behavior of the RR Lyrae stars in the Galactic bulge sample of the OGLE project, Moskalik (2000, hereafter M00) also found several variables with closely spaced frequencies. Furthermore, in a selectively chosen sample of the MACHO RR Lyrae inventory, Kurtz et al. (2000) also picked a few amplitude- and phase-modulated (Blazhko-type) variables among the first overtone stars.

In the present paper we carry out a *systematic* study of the frequency spectra of 1350 first overtone stars of the MACHO project for the Large Magellanic Cloud. The results of the investigation of a shorter segment of the same data set have already been briefly summarized by Kovács et al. (2000). This is the first large-scale survey of the finer details of the temporal behavior of the variable star data of a microlensing survey. (We note however, that in a recent paper, Udalski et al. 1999, without going into the details, mention a similar massive analysis in a search for double-mode Cepheids in the Small Magellanic Cloud.) Due to the large size of the sample, this study also yields valuable statistics in respect of the occurrence rate of the various modal behaviors among first overtone stars. This, together with other information on the fundamental mode RR Lyrae stars, supplies crucial observational data for understanding RR Lyrae pulsation, and, in particular, the Blazhko phenomenon.

Because of the various pulsation behaviors discovered among RR Lyrae stars, we found it necessary to introduce new notation for the already known classical types. Throughout this paper we use RR0 for fundamental, RR1 for first overtone and RR01 for double-mode (fundamental & first overtone), instead of the traditional notation of RRab, RRc and RRd. We will see that the new notation can be more successfully adapted to label new types and subtypes of variables.

2. THE DATA AND THE METHOD OF ANALYSIS

The analysis presented in this paper utilizes the data obtained during the *first 6.5 years* of the MACHO project. The primary selection of the sample was made through a cut in the color-magnitude diagram from the fields observed by the project (see <http://wwwmcho.mcmaster.ca>). The magnitude and color ranges were confined in the $18.5 \geq V \geq 20.0$ and $0.5 \geq V - R \geq 0.1$ intervals. This set was tested for variability by employing various statistics of the magnitude distributions of the individual objects. Next, the time series of the candidate variables were passed through a period search algorithm. In the final step of the primary selection the folded light curves were examined to filter out eclipsing binaries and other variables different from RR1 stars. Since the present sample contains variables only from 17 out of the 30 fields observed by the project, the sample is not complete. From the number of all variables (of any type) in the 30 fields and from the occurrence rate of RR1 variables in the 17 fields analyzed, we estimate the completeness to be 52%. Details of the MACHO image and photometry data are provided in Alcock et al. (1999).

Since our interest is focused only on the temporal behavior of the variables, in our primary survey we employ only the *instrumental 'r' magnitudes*. However, when this color leads to dubious results, we also examine the frequency spectra corresponding to color 'b'. Although the present RR1 sample contains about 1350 variables, some overlaps exist among the various fields both within this set and also with some of the 73 RR01 stars discovered by Alcock et al. (1997, hereafter A97).

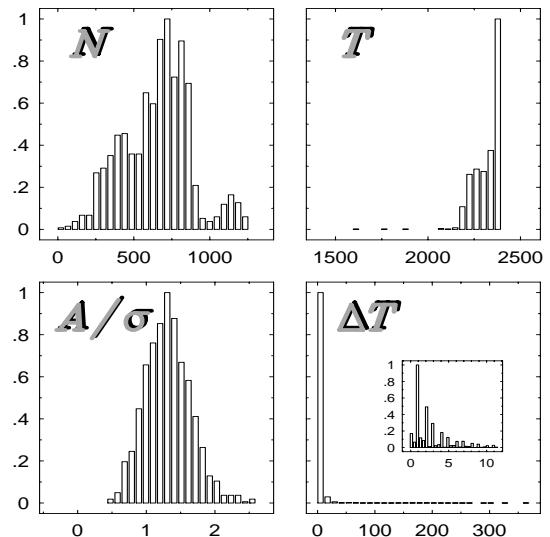


Fig. 1 – Distribution functions of the various time-series parameters of the RR1 sample. *Upper left*: number of data points; *upper right*: total time span (in [days]); *lower left*: signal to noise ratio (see text); *lower right*: sampling time (in [days]). The inset shows the fine details of the ΔT distribution under 10 days. The highest peak of each distribution function is normalized to 1.

Further details on the data lengths, temporal distributions and signal to noise (S/N) ratios are given in Figure 1. We

see that the most probable number of data points per variable is between 600 and 800 and is rarely less than 250, whereas for a considerable number of stars it exceeds 1000. The length of the total time span T peaks at 2370 d which corresponds to the above mentioned 6.5 yr duration. Because of observational schedule, some of the variables cover a shorter time span, but very few of them extend for less than 6 yr. In the lower right corner we plot the distribution of the sampling time $\Delta T = t_{i+1} - t_i$. Because the LMC is circumpolar at Mount Stromlo, the data window is free from any long-term periodicity. The most significant problem comes from the daily sampling, but even this alias is tamed by the slight irregularity in the sampling rate as is exhibited by the small peaks between zero and 2 d in the distribution function. All these result in spectral windows which can be, in general, easily tackled as we will see in the subsequent sections.

To characterize the noise properties of the light curves we define the signal to noise ratio A/σ as the ratio of A , the amplitude of the first component of a 3rd order single-period Fourier fit, to σ , the standard deviation of the residuals of this fit. In the distribution function of A/σ , in the lower left corner of Figure 1, we see that the size of the noise is comparable to the main signal amplitude. Since only some 30% of the total RR1 sample is multiperiodic (see later), the observed low S/N ratio is indeed due to the high noise, and not to the excess scatter attributed to secondary signal components. In some cases the light curves have substantial higher harmonic components, and, therefore, the total amplitudes might be twice of that of the first Fourier component, which results in a better S/N ratio.

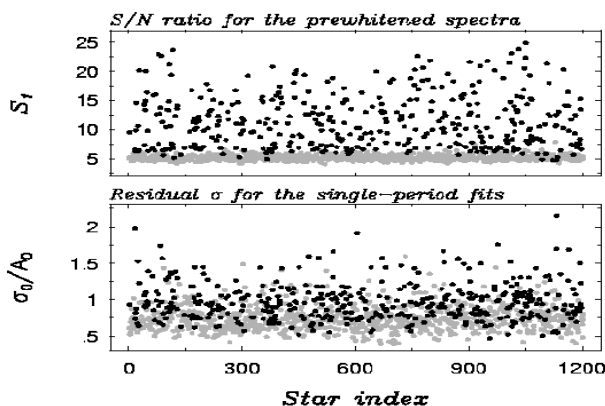


Fig. 2 – Efficiency of searching for secondary signal component through Fourier frequency analysis of the prewhitened data (*upper panel*) and through the residual scatter of the single-period fits (*lower panel*). *Gray dots* show the monopерiodic, *black dots* show the multiperiodic variables. Stars are listed by some registration index.

At such a low S/N ratio, when searching for secondary signal components, it is crucial to perform a frequency

analysis combined with a *prewhitening* technique. During the prewhitening cycles we successively subtract the corresponding highest amplitude signal component and its first two harmonics from the time series. The fact that examination of the residual scatter in a single-period fit is *not* a decisive test for detecting secondary signal components in the low S/N case, is demonstrated in Figure 2. By using the observed data, in the lower panel we plot the relative residual scatter for the signal before the first prewhitening. Here σ_0/A_0 is the reciprocal of the same quantity plotted in Figure 1 (we use the zero subscript only to emphasize that the quantities refer to the data before the prewhitening cycles). We see that the multiperiodic stars are intermingled with the monopерiodic ones and only a few of them stand out relatively well from the rest of the sample.

For characterizing the S/N ratio of the prewhitened spectra, the following quantity is introduced

$$S_1 = \frac{A_p - \langle A(\nu) \rangle}{\sigma_{A(\nu)}} . \quad (1)$$

Here A_p is the peak value in the amplitude spectrum, $\langle A(\nu) \rangle$ is the frequency-averaged value of the spectrum, $\sigma_{A(\nu)}$ is the standard deviation of the amplitude spectrum in the given band width. The plotted values are obtained by considering the $[0.5, 5.5] \text{ d}^{-1}$ frequency band. We see that most of the detections are rather safe, with confidence limits better than 6σ . It is clear that in future automatic search for multiperiodic variables statistics S_1 could be very helpful.

The frequency analysis is carried out by employing a standard Discrete Fourier Transformation (DFT) for unequally spaced data (see e.g., Deeming 1975). The input time-series of the DFT is obtained by subtracting the average from the original data set and omitting 4% of the data points which have the largest deviations from the average. We take the $[0.5, 5.5] \text{ d}^{-1}$ frequency band for the primary survey and the $[0.0, 6.0] \text{ d}^{-1}$ band for the detailed analysis of the multiperiodic cases. All spectra in the above bands are calculated with 60000 and 80000 frequency steps, respectively. To avoid plotting unimportant features and unnecessarily large arrays, we employ *economic plotting*, which means that the plotted values correspond to the maximum amplitudes in the bins of the chosen bin resolution of the total frequency band. The number of bins in our case is 2000. In each prewhitening cycle the location of the highest peak in the given band width is used to calculate a more accurate estimation of its frequency. This is done by a least-squares technique, by searching for the minimum dispersion around a 3rd order single-period Fourier-sum. Up to three prewhitening cycles are performed in the multiperiodic cases. All spectra and folded light curves are *visually* inspected and then *classified according to the prewhitened spectra*. As we see from the statistics of S_1 in Figure 2, in principle one could pick up most of the multiperiodic variables on the basis of the $\approx 6\sigma$ criterion. However, at this stage of the analysis of a still ‘reasonably’ low number of variables, the ‘manual’ search is preferred in order to ensure that no interesting cases are missed because of slightly marginal detectability. Finally, in the class of variables showing period change, we employ a very simple time-dependent Fourier analysis,

which consists of a series of single-period Fourier fits to the adjacent parts of the time series.

3. RR01-TYPE STARS: VARIABLES WITH THE FUNDAMENTAL & FIRST OVERTONE MODES

This class of variables is the simplest to detect in the present data set. The standard prewhitening method

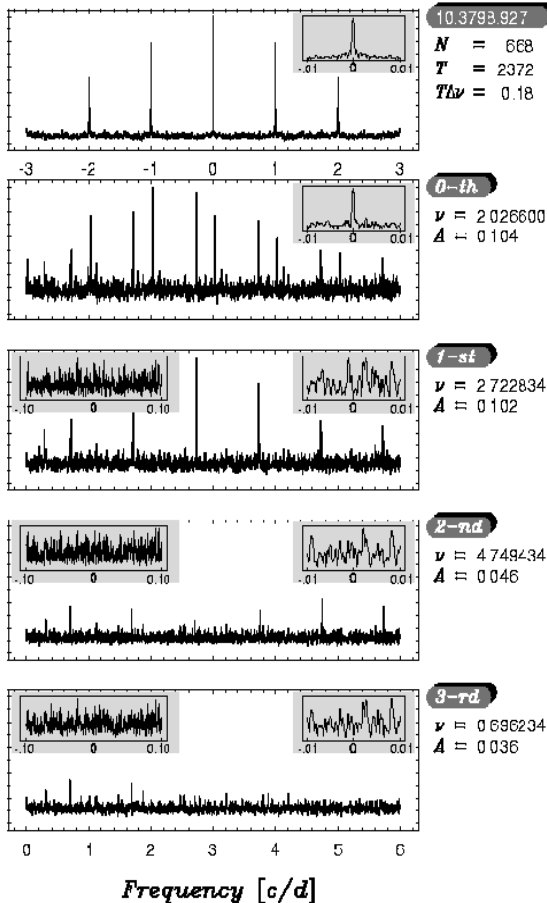


Fig. 3 – Example of the detection of a double-mode (RR01) variable. The upper panel shows the spectral window. Inset displays the fine structure around the main peak. Label shows the MACHO identifier, number of data points (N), length of the total time span (T in [days]) and frequency resolution ($T\Delta\nu$) of this and all the following wide frequency band spectra. Subsequent panels show the amplitude spectrum of the original data and the results of the corresponding prewhitening cycles (see Sect. 2 for details). Insets show the fine structure of the spectra centered around the main peak of the spectrum of the original data. Labels show the prewhitening order, the frequency and the amplitude (in d^{-1}) and in MACHO ‘r’ magnitude, respectively) of the main peak of the corresponding prewhitened spectra. The wide frequency band spectra are normalized relative to the highest peak in the spectrum of the original data. The spectra shown in the insets are normalized separately to the highest peaks in the narrow frequency band of the corresponding spectra. As it is described in the text, economic plotting is employed in all cases.

based on the maximum peak subtraction almost always works, although we use a wide frequency band and do not

restrict the search to some ‘proper’ period ratio regime. This latter condition is applied only in one or two cases from the 156 successful searches. (We note, however, that 48 stars from this set are either doubly identified or have already been discovered by A97, using a reduced and different data set.) In many cases the lowest order combination frequencies $f_1 - f_0$ and $f_1 + f_0$ are also identified (the harmonics are automatically subtracted by our 3rd order monoperic fits). Figure 3 illustrates the case when these combination frequencies are easily visible. We draw attention to the following important features: (a) the spectral window contains only the integer d^{-1} aliases, and is free from any long-term alias problems (this property is true for almost all time series); the 1 d^{-1} aliases are sufficiently small and in most cases do not hamper the identification of the maximum peak in the spectra; (b) the combination frequencies are very well reproduced from f_0 and f_1 , which is a strong indication of the physical nature of the frequencies found. The basic parameters of the previously unknown RR01 variables are given in Table 1¹. (The amplitudes A_1 and A_0 refer to the first overtone and fundamental modes, respectively, and are obtained through monoperic Fourier fits during the prewhitening procedure. The coordinates refer to the year 2000.) Together with the already published variables by A97, there are 181 RR01 stars known in the LMC. This number of variables is about three times of the total number of RR01 stars presently known in globular clusters, galaxies and in the Galactic field.

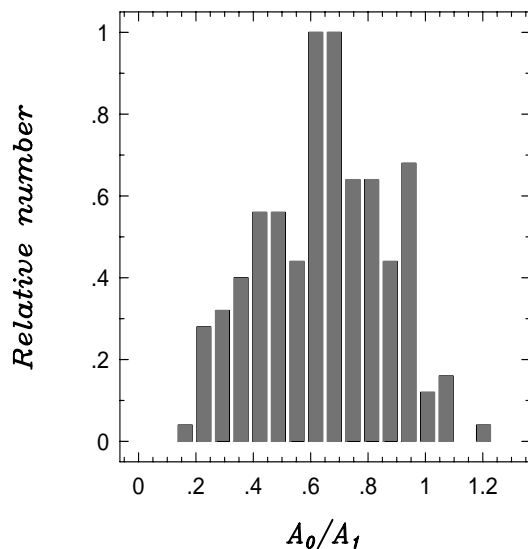


Fig. 4 – The distribution of the fundamental to first overtone amplitude ratios for all the 181 RR01 stars in the LMC.

When plotted either on the period–amplitude or on the period–apparent magnitude diagrams, LMC RR01 stars do not seem to be distinguishable from the single-mode RR1 stars. They occupy a relatively narrow period range of $0.33 \text{ d} < P_1 < 0.41 \text{ d}$ (there is only one star with $P_1 = 0.43 \text{ d}$).

As it is shown in Figure 4, the ratio of the amplitudes of the two modes shows a wide range, but the fundamental mode amplitude A_0 rarely exceeds that of the first over-

¹Tables 1 – 6 are presented after the REFERENCES

tone. Apparently there is a lower cut in the A_0/A_1 ratio at 0.2, because we do not observe lower ratio than this, although our detection limit is below this value (see the tests for the Blazhko variables in Sect. 5).

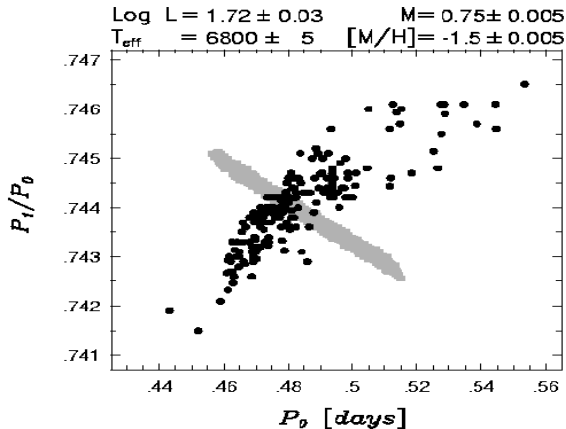


Fig. 5 – Position of the LMC RR01 stars in the $P_0 \rightarrow P_1/P_0$ diagram. For comparison, we also show by gray-colored background the area occupied by models selected in the parameter regime shown in the header. The models of Kovács & Walker (1999) are used with the OPAL’96 opacities. The Hydrogen abundance X is fixed at 0.76 and the adopted value of the solar metallicity Z_\odot is 0.02. Mass and luminosity are given in solar units.

It is well known that the $P_0 \rightarrow P_1/P_0$ diagram (Petersen 1973) carries important information about the metal content and mass of the RR01 stars (Kovács, Buchler & Marom 1991). In Figure 5 we plot this diagram for all known LMC RR01 stars, together with the region of the models occupied at some fixed metallicity and mass. It is seen that the constant mass and metallicity assumption is not applicable to the whole RR01 population of the LMC. Assuming that either the mass or the metal content is the sole agent for the observed topology, we get rough estimates of $\pm 0.15 M_\odot$ and ± 0.3 dex, respectively, necessary to cover the total ranges of periods and period ratios. There is also a dependence on L and T_{eff} which influences the applicable average values of mass and $[M/H]$ (in the case displayed we use the so-called ‘brighter’ luminosity scale – see Kovács & Walker 1999). It is obvious that the proper treatment of this problem requires additional information, most importantly accurate abundance values of the LMC RR01 variables. For further discussion of this problem we refer to A97, Popielski & Dziembowski (2000) and Clementini et al. (2000).

4. RR1- ν 1-TYPE STARS: VARIABLES WITH 2 CLOSELY SPACED FREQUENCIES

These variables represent a special type of double-frequency pulsation. The frequency ratios are always larger than 0.95 and could be as large as 0.999. In Figure 6 we show an example for the patterns obtained in the case

of medium frequency separation. It is clear that in the frequency band analyzed, there are no other components except for the 2 closely spaced ones we identified. (As it is seen in the third panel, the nearly equidistant triplet structure of the low-frequency aliases is due to the power leakage from negative frequencies.) Other solutions, such

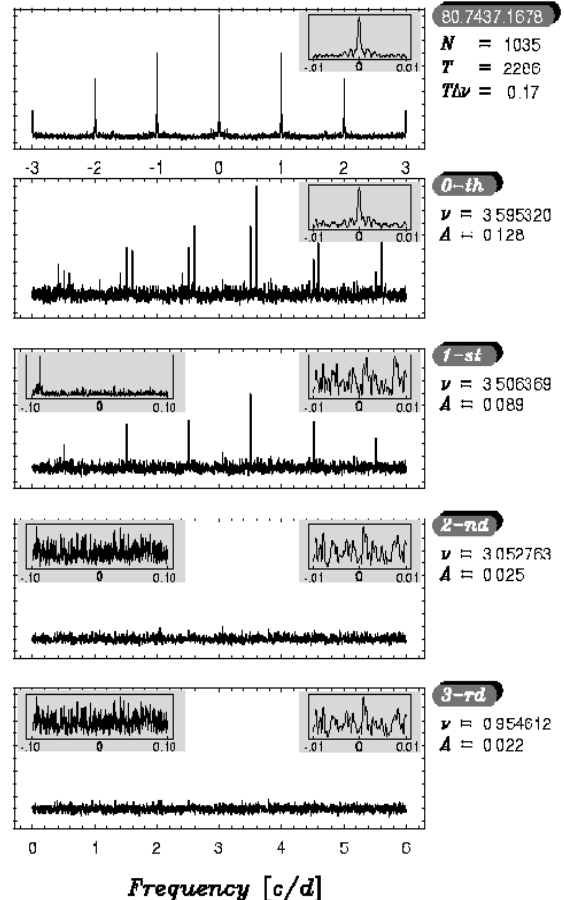


Fig. 6 – Detection of an RR1- ν 1 variable (RR1 star with 2 closely spaced frequencies). Notation is the same as in Figure 3.

as the RR01 frequency pattern are not possible, both because of the fairly clear alias patterns obtained during the calculation of the present solution, and also because on physical grounds (i.e., we would have obtained ‘bad’ period ratios with the RR01 assumption). Unlike in the case of Galactic bulge RR0- ν 1 variables analyzed by M00, we do not find traces of the combination frequencies $\nu_1 - \nu_0$ and $\nu_1 + \nu_0$. There is only one variable with frequency separation smaller than $0.01 d^{-1}$ (see Figure 7). The status of this star is slightly ambiguous, because the ‘b’ data suggest the presence of a symmetric frequency pattern (see next section), although the feature is sufficiently hidden in the noise, similarly to the case of the ‘r’ data shown in the figure.

The main properties (frequency ν_0 and amplitude A_0 of the main – i.e., higher amplitude – component, frequency separation $\nu_1 - \nu_0$, and the ratio A_1/A_0 of the secondary and main amplitudes) of the 24 RR1- ν 1-type variables are listed in Table 2. Most of these stars have frequency separations between 0.01 and $0.1 d^{-1}$ and only a few of

them exceed these limits. 63% of the variables have negative frequency differences (i.e., the secondary, lower amplitude component has smaller frequency than the main component). In the case of positive frequency difference the secondary amplitudes are almost always quite comparable with those of the main components. It is also seen that the period regime in which RR1- ν 1-type pulsations occur, is fairly wide.

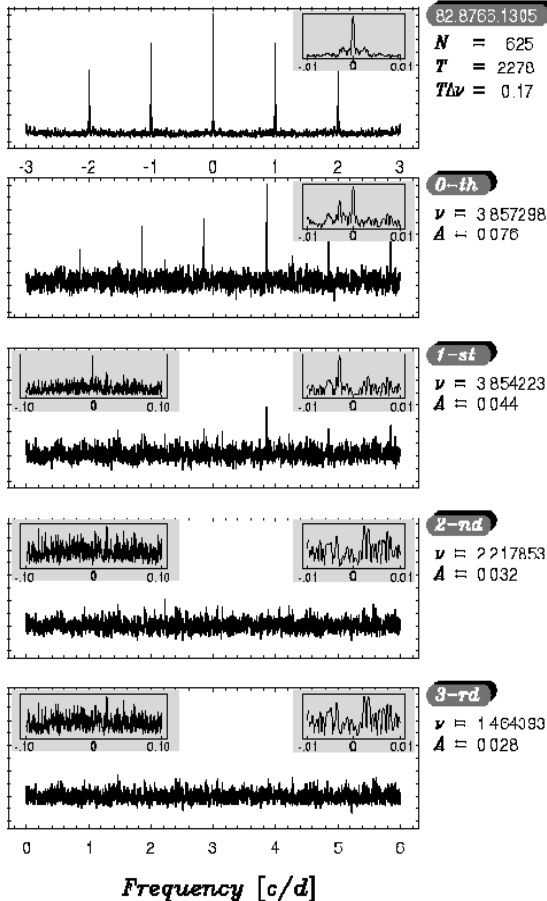


Fig. 7 – RR1- ν 1 variable with small frequency separation. For notation, see Figure 3.

For a closer inspection of the overall properties of the RR1- ν 1 spectra, in Figures 8 and 9 we show a representative sample of this type of variables. In many cases the secondary components are very easily visible even without prewhitening. In some prewhitened spectra of sufficiently low noise level, one may suspect the presence of additional low-amplitude components. Specially interesting are those in which the suspected component forms a symmetric triplet with the main and secondary components. As an example, we recall the case of 82.8766.1305 (see note to Table 2), where the ‘b’ data support the existence of such a symmetric frequency pattern. On the other hand, a closer examination of the suspected third component for 2.5266.3864 reveals that it is asymmetric and becomes very small after the second prewhitening, whereas for 80.6352.1495 the very marginal possible third component indicated in Figure 9 completely disappears. These conclusions are also supported by the analysis of the ‘b’

data. We return to the problem of hidden symmetric frequency patterns in the next section during the discussion of the Blazhko variables.

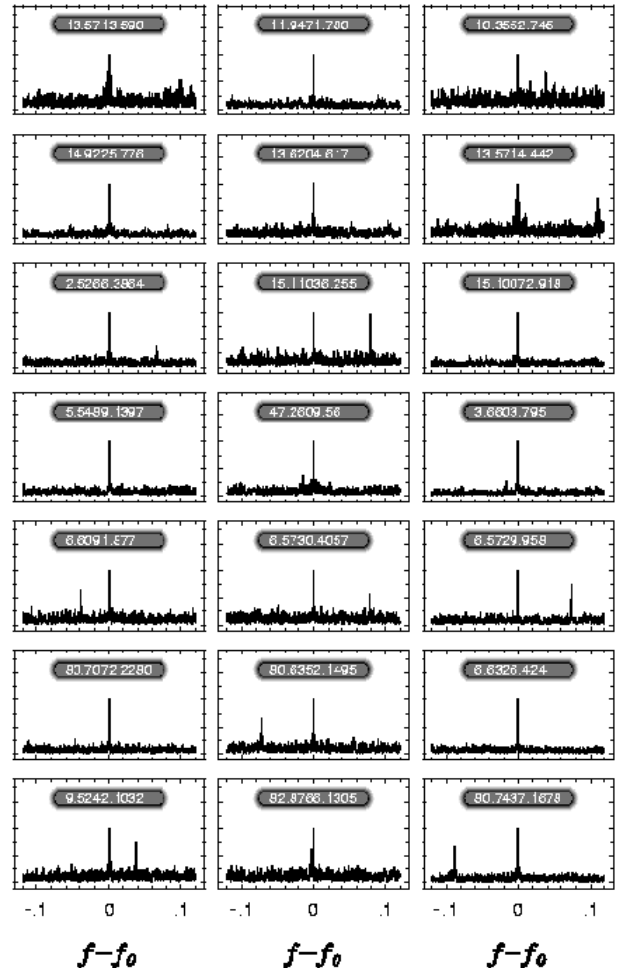


Fig. 8 – Amplitude spectra of a sample of RR1- ν 1 stars without prewhitening. Each spectrum is normalized to the same level by the corresponding highest peak.

As we have already mentioned in Sect. 1, parallel with the present study, RR1- ν 1-type variables have also been discovered in other stellar systems. There are 3 RR1- ν 1-type stars in the globular cluster M55, 1 in M5 (O99a,b) and 2 in the OGLE-sample of 66 RR1 stars of the Galactic bulge (M00). It is worthwhile to mention that for four of these variables the frequency difference is negative in agreement with most of the values in our sample. In addition to the two RR1- ν 1-type stars, M00 found similar type of stars in the RR0 population. From the 149 stars he identified 11 variables with two closely spaced frequencies. It is interesting to note that 9 of these stars have frequency spacings with opposite sign to that of the majority of the RR1- ν 1 stars. The authors of both of these papers argue strongly that these discoveries are the first observational proofs for the existence of *nonradial modes* in RR Lyrae stars. Indeed, it is difficult to escape this conclusion, especially in the light of the recent theoretical works indicating the excitation of nonradial modes in RR Lyrae stars

(Van Hoolst, Dziembowski & Kawaler 1998; Dziembowski & Cassisi 1999).

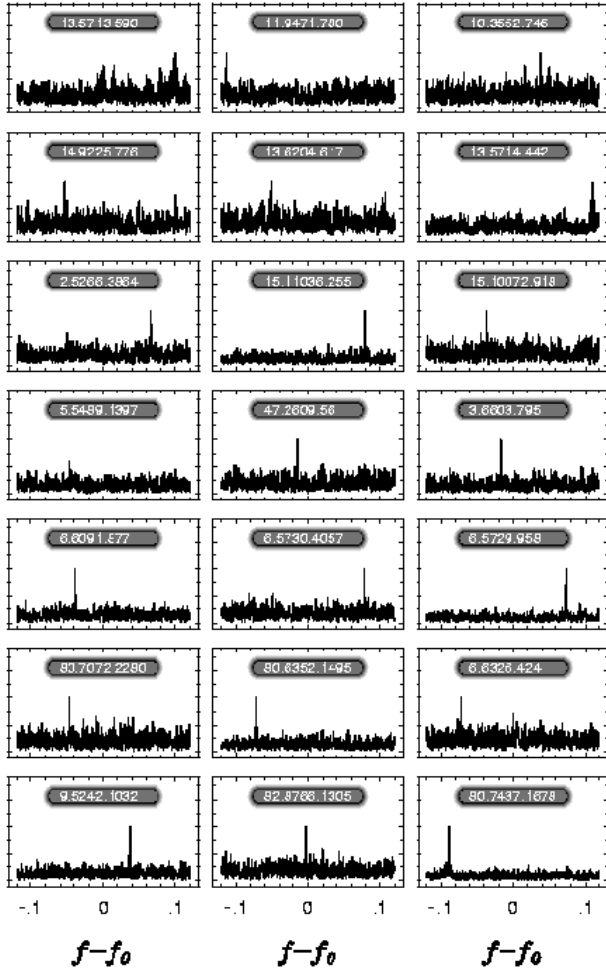


Fig. 9 – Amplitude spectra of a sample of RR1- ν 1 stars for the data after the first prewhitening. Each spectrum is normalized to the same level by the corresponding highest peak.

5. RR1- BL -TYPE STARS: VARIABLES WITH 3 SYMMETRICALLY SPACED CLOSE FREQUENCY COMPONENTS

Fourier analyses of Galactic field RR0 stars with Blazhko effect (Borkowski 1980; Smith et al. 1994, 1999; Kovács 1995; Nagy 1998; Szeidl & Kolláth 2000) revealed a very simple frequency pattern for these stars. The spectra constitute a sequence of *equidistant triplets*, centered around the fundamental mode frequency and its harmonics. This structure can be observed up to the 5th – 7th harmonics. The frequency spacing corresponds to the modulation (Blazhko) period. The amplitudes of the modulation components around the harmonics are 10–30% of the corresponding harmonics and are, in general, not symmetric. Their contributions add up in the directly observable amplitude and phase changes and result in considerable amplitude variations of 30–50% (Szeidl 1988).

Before the present analysis (see also Kurtz et al. 2000) it was unclear whether Blazhko-type modulation was also

present in RR1 stars. Interestingly, we find that this behavior does also occur in RR1 stars; however, its incidence is much lower than among RR0 stars. We discovered altogether 28 variables showing Blazhko-type frequency patterns. The details of the prewhitening procedure for such a variable are shown in Figure 10. Again, here we draw the attention to the flat spectrum after prewhitening by all three peaks. Equal frequency spacing is also well displayed. Although most of the variables have modulation frequencies similar to the example shown, 7 variables have rather small ones, corresponding to modulation periods longer than 600 d. In Figure 11 we show an example for such a variable. It is seen that despite the very small separation, the components are still clearly resolved due to the long baseline of the data.

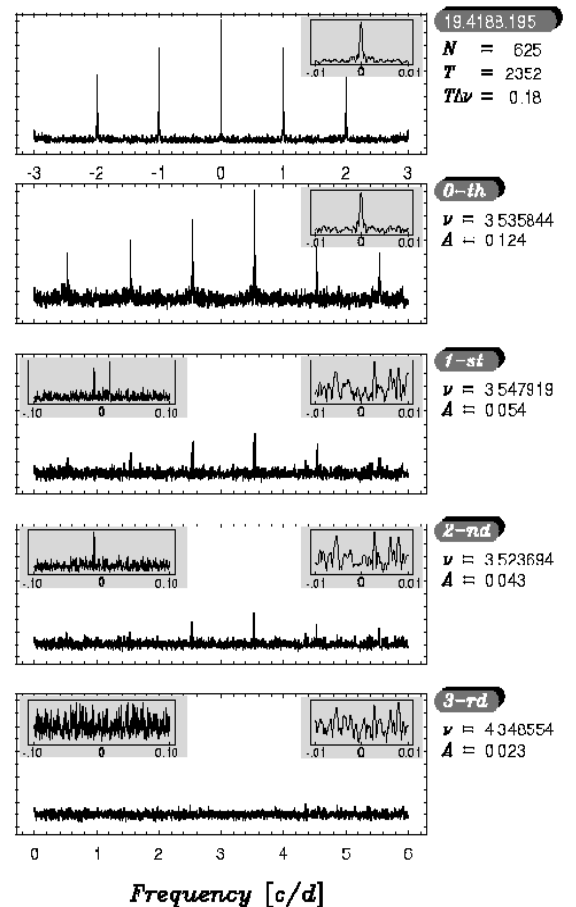


Fig. 10 – Detection of a first overtone Blazhko variable (RR1 star with 3 symmetrically spaced close frequencies). Notation is the same as in Figure 3.

The results of the analysis for the RR1- BL -type variables are summarized in Table 3. The quantities corresponding to the highest peak in the frequency spectrum before prewhitening are labeled with zero subscripts. The + and – signs denote components which have, respectively, larger and smaller frequencies than the main component (i.e., $\Delta f_{\pm} = \nu_{\pm} - \nu_0$). We see that except for 11.9355.1380, in all cases the main component is also the center of the

triplet. The lowest and highest detected modulation levels are 12% and 82%, respectively.

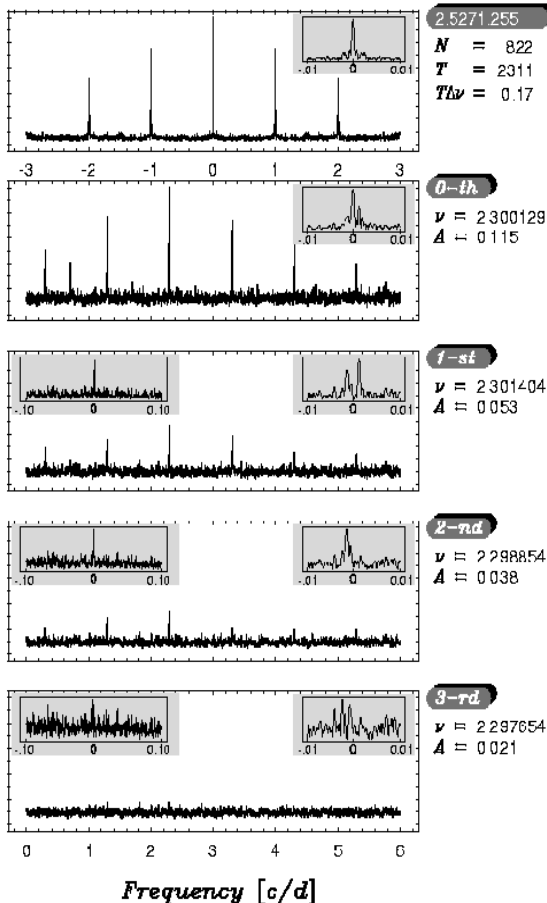


Fig. 11 – Blazhko variable with very small frequency separation. For notation, see Figure 3.

For an overview of the patterns of the RR1–BL-type frequency spectra, in Figures 12 and 13 we display the spectra of the data before and after the first prewhitening. In some cases we see remnants precisely at the ν_0 component. These are either due to long-period modulations not resolved on the present plotting scale, or to period changes of the main components. Furthermore, in other cases, the presence of additional close component(s) can also be suspected (e.g., 82.8765.1250).

In the following we address two questions which are important for the physical models of the Blazhko phenomenon: (a) What is the statistical significance of the slight deviations from equidistant frequency spacing? (b) How small is the lowest observable level of modulation in the present data set?

Problem (a) is tested in the following way. For each variable to be tested for the significance of the equidistant frequency spacing, we generate a synthetic signal by using the average of the observed frequency distances and the corresponding Fourier decomposition obtained from fitting this equidistant frequency triplet to the data. Then Gaussian noise is added to this signal with the standard deviation of the residuals of the Fourier fit of the original data mentioned above. After analyzing many realizations of the

so-obtained time series, we check the statistical properties of the calculated frequency distances. The deviation from

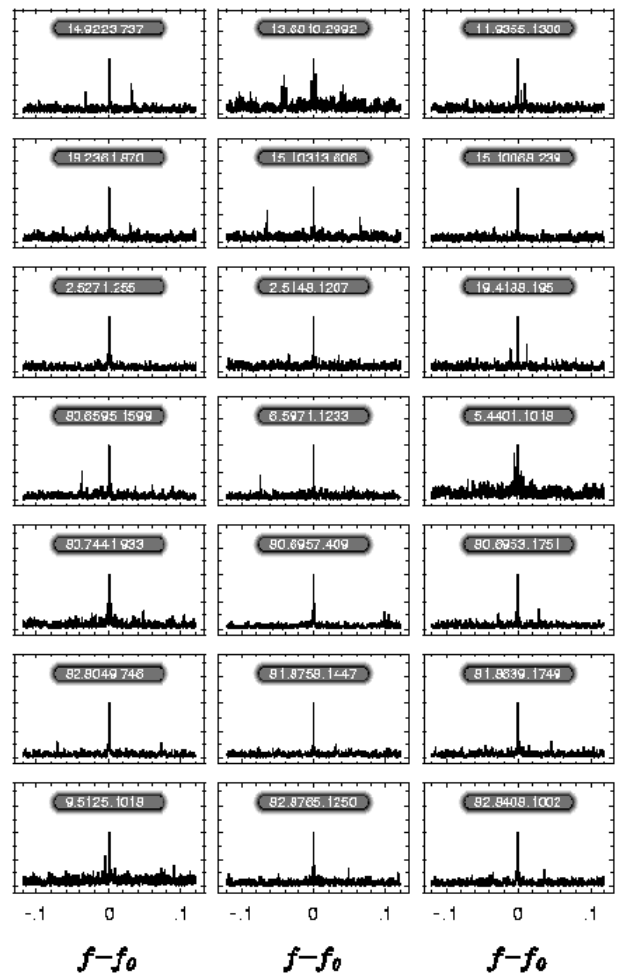


Fig. 12 – Amplitude spectra of a sample of Blazhko stars without prewhitening. Each spectrum is normalized to the same level by the corresponding highest peak.

the equidistant pattern is measured by the absolute value of the difference between the two spacings, i.e.,

$$\delta f = |\Delta f_+ + \Delta f_-| . \quad (2)$$

In Figure 14 we show the empirical probability distribution of δf for one of the variables in Table 3. We see that the observed deviation is well within the probability limit expected from the effect of observational noise. The same conclusion is drawn from the tests performed with other variables.

Turning to problem (b), we see from Table 3 that the modulation level $A_{\pm}/A(\nu_0)$ for most of the RR1–BL variables is larger than 20%. We have only one variable for which both components are under this limit. The question of lowest modulation level is important from the point of view of the relation between the Blazhko RR0 and RR1 stars, because the possibility of the existence of RR1 stars with low-level modulation would increase the number of Blazhko RR1 stars, thereby decreasing the gap between the occurrence rates of the two classes of Blazhko variables.

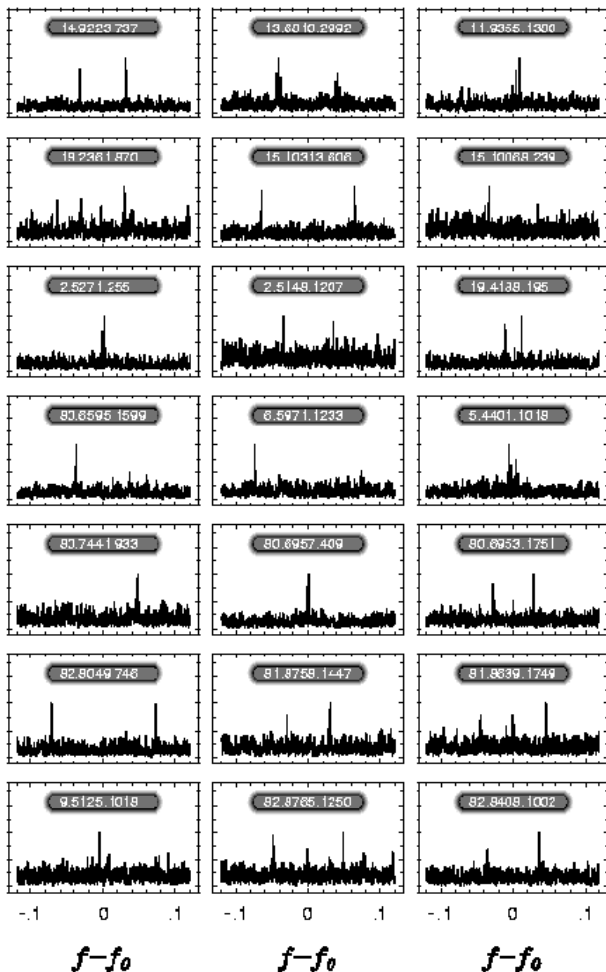


Fig. 13 – Amplitude spectra of a sample of Blazhko stars for the data after the first prewhitening. Each spectrum is normalized to the same level by the corresponding highest peak.

To clarify this question, the following tests are performed. First, we select high S/N ratio stars from the monoperoic RR1 variables. Stars which satisfy the $(0.16A(\nu_0) - \langle A(\nu) \rangle) / \sigma_{A(\nu)} > 5.0$ criterion are chosen for the test. Here $A(\nu_0)$ denotes the amplitude of the observed main component, other symbols have the same meaning as in Eq. (1). This condition is in line with the detection properties of the secondary components discussed in Sect. 2 and implies a modest or good chance to find any secondary components with amplitudes greater than 16% of the corresponding main components. We note that the number of stars selected with this method is a very sensitive function of the required discrimination/detection limits. For example, with the above criterion we get 216 variables, whereas with a 15% limit we get only 140.

In the next step each time series is prewhitened by the main component. Then, two symmetric components are added to the residuals with $A_{\pm}/A(\nu_0) = 0.10$ or, in another test, with $A_{\pm}/A(\nu_0) = 0.15$. In both cases $|\Delta f_{+}| = |\Delta f_{-}| = 0.04$ and the phases are arbitrary but equal. The resulting time series is analyzed through three sequential prewhitenings in the $[\nu_0 - 0.12, \nu_0 + 0.12]$ d^{-1}

band, and searched for significant peaks (both visually and automatically, by finding the most symmetric triplets from the four frequencies with the highest amplitudes).

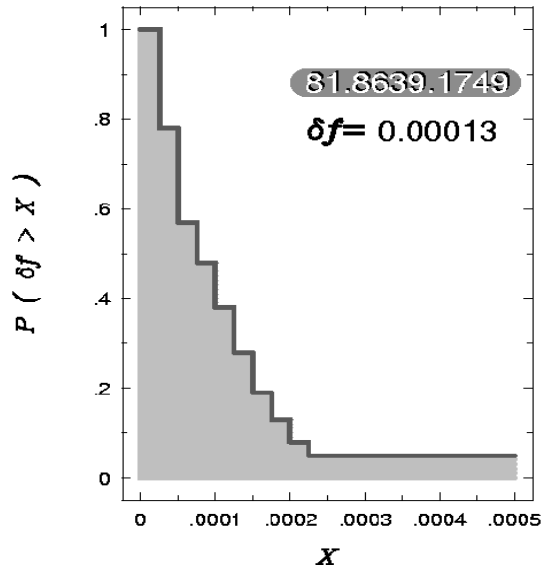


Fig. 14 – Empirical probability distribution function of the deviation from equidistant frequency pattern due to observational noise. The observed deviation is given in the top right region of the figure under the variable identification code.

By allowing a maximum frequency asymmetry of $\delta f = 0.001 \text{ d}^{-1}$, in the $A_{\pm}/A(\nu_0) = 0.15$ test we find 155 cases where the two symmetric peaks can be identified. In the case of weaker secondary components ($A_{\pm}/A(\nu_0) = 0.10$), we still have 49 successful identifications based on the existence of symmetric triplet structures among the four highest peaks obtained during the prewhitening sequences. A ‘conservative’ visual examination of the spectra after the first prewhitening leads to a similar conclusion. In the test of 10% modulation level we find 49 cases where only one significant component is seen (6 of them do not appear at the test frequency). In 22 additional cases we see clear equidistant triplet structures. It is evident that if we assume a 20% occurrence rate of these Blazhko stars with low-level modulation, in this limited sample of 216 stars alone we should have seen more than $0.2 \times (49 + 22) = 14$ of them either as RR1- ν 1 or RR1- BL variables.

In Figure 15 we display some of the spectra to visualize the significance of the detection of the side components in the test case of the 15% modulation level. From the 30 cases shown, there are only two in which none of the components are readily visible.

Considering only the test results of the automatic search for triplet structures, let us assume that the incidence of the RR1- BL stars with these low-amplitude modulations follows the rate of $\approx 20\%$ found for the RR0 stars. Then, with the minimum amplitude modulation of 10%, the conservative estimate is that we expect at least some $49 \times 0.2 \approx 10$ additional RR1- BL stars in the original data set. (With the 15% minimum modulation level this

number would increase to 31.) To test if we have missed some faint close components during the basic screening of

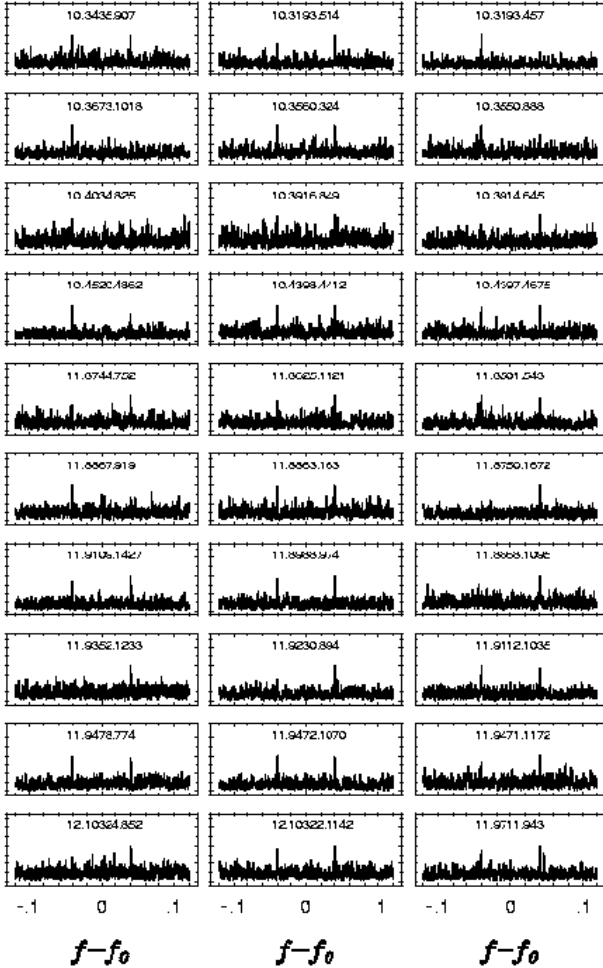


Fig. 15 – Amplitude spectra of a sample of the **test signals** after the first prewhitening. The **artificial side components** correspond to 15% modulation level. Each spectrum is normalized to the same level by the corresponding highest peak.

the data, we repeat the above analysis on the original data, without the injection of the faint secondary artificial signal components. A visual inspection of the spectra of the 216 stars confirms our first conclusion, namely, these stars are indeed monophasic variables. In Figure 16 we show the 12 best cases, where a search for symmetric triplet structure among the highest peaks indicates the presence of such hidden triplets. Comparing with the examples of the 15% test signal case, we see that even these ‘best’ cases are of very low statistical significance. From these tests we conclude that if RR1–BL stars with low modulation levels of 10–15% exist at a rate more than 10%, we should have found such stars in a significant number. It seems rather probable that the incidence of the Blazhko stars among the LMC RR1 stars cannot be larger than a *few percent*.

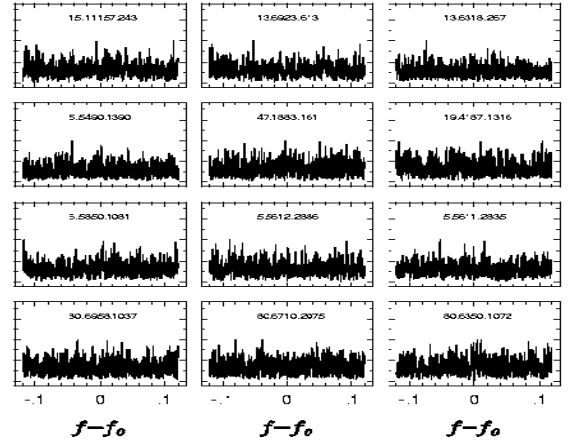


Fig. 16 – Amplitude spectra of a sample of monophasic variables after the first prewhitening. For these variables a numerical search for hidden symmetric frequency triplets led to positive results. Each spectrum is normalized to the same level by the corresponding highest peak.

6. RR1–PC-TYPE STARS: VARIABLES WITH PERIOD CHANGES

In the course of the basic scan of the variables, we found a considerable number of stars whose prewhitened frequency spectra contained significant remnant power very close to the main component. Due to the proximity and unresolved nature of these remnants, we attribute their existence to long-term period and/or amplitude changes. Quite often the phenomenon can also be recognized by the broadening of the line profiles in the frequency spectra. Because of the non-discrete nature of the frequency spectra, the standard prewhitening procedure does not work in these cases. In Figure 17 we show an example of the failure of successive prewhitenings. Spectral line broadening is also well observable in the present case.

For a closer examination of the nature of the long-term variation, we perform the following *simple time-dependent Fourier analysis*. A sequence of single-component Fourier fits is calculated on overlapping segments of the time series by shifting the base of the fit by one item of data in each step. The length of the base of the fits is chosen to ensure reasonable stability in the calculated time-dependent amplitudes and phases when the base-length is increased. In most cases we reach this situation by choosing 50–100 data points per segments. We also test two simple mathematical models of the long-term modulation. The first one consists of a linear period change of the main component

$$P(t) = \langle P \rangle + \beta(t - t_0) , \quad (3)$$

where $\langle P \rangle$ is a properly chosen average period, t_0 is an arbitrary epoch and β is the rate of period change. We expect this model to work well when the phase variation

derived above is closest to a second order polynomial. The second model assumes a pure exponential modulation in the following form

$$A(t) = \langle A \rangle e^{\eta(t-t_0)}, \quad (4)$$

where $\langle A \rangle$ is some average amplitude.

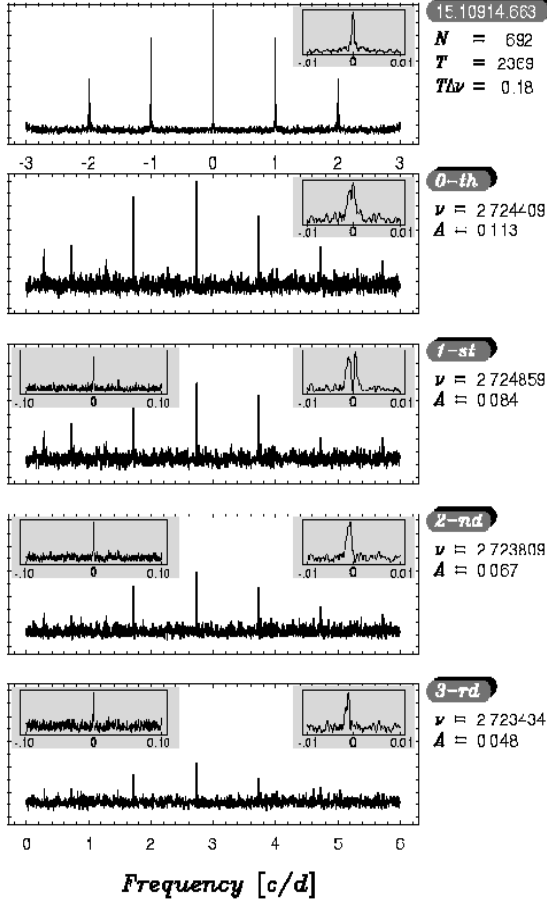


Fig. 17 – Detection of an RR1-PC variable (RR1 star with unresolved components at the main frequency). For notation, see Figure 3.

After performing these tests on the 141 RR1-PC variables, we find that *none* of them can be modeled by the assumption of pure exponential amplitude change. On the other hand, the model of linear period change works better in a significant number of cases. However, the time-dependent Fourier analysis reveals that for most of the RR1-PC variables these simple models are unable to give a full account of the observed remnant power in the frequency spectra. In Figure 18 we show representative cases for the almost pure linear period change and for the more general situation when this simple description is not applicable. It is important to remark that the present simplified time-dependent analysis can be regarded as very preliminary, because the high noise level and the strong period change would require the application of a more sophisticated method. For instance, tiny amplitude changes (if they exist), are certainly not detected with this method due to the large errors of the calculated amplitudes from the short data segments in the presence of such a

high noise. However, the observed phase changes seem to have much higher significance because of the considerable range of phase variations associated with them. In addition, a comparison with a similar analysis performed on some RR1 variables reveals that indeed, they show irregular/noisy phase variations several times smaller. At the same time, their temporal amplitudes behave very similarly to those of the RR1-PC stars.

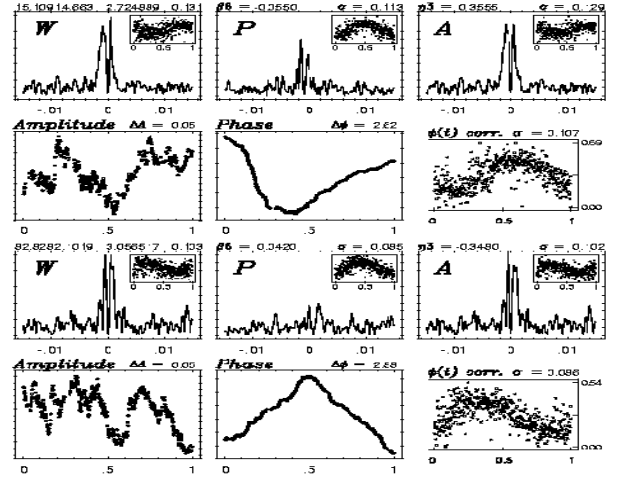


Fig. 18 – Results of the various tests performed on two RR1-PC-type variables. *Uppermost row:* whitened spectra calculated in the regime of the main component with the assumptions of $P = \text{const.}$ (W), linear period change (Eq. (3), P) and exponential amplitude change (Eq. (4), A). All spectra are normalized by the highest peak of the W spectrum. *Insets:* corresponding folded light curves. *Headers:* star code, main frequency [d⁻¹], σ [‘r’ mag] of the folded light curve, $\beta_6 = \beta \times 10^6$ [d⁻¹], $\eta_3 = \eta \times 10^3$ [d⁻¹], the sigmas refer to the folded light curves obtained by the corresponding assumptions. *Next row:* time-dependent amplitude, phase and folded light curve corrected by the plotted phase variation. The horizontal axes in the first two figures represent the total time span. *Headers:* the total amplitude and phase ranges shown, σ of the folded light curve. *Subsequent rows:* as above, but for a different variable.

We draw the attention to the fact already mentioned, namely that a simple exponential amplitude variation cannot explain the remnant power in the spectrum. Furthermore, the light curves corrected for the phase variation show considerably lower scatter. For these reasons we refer to the above class of variables as PC (period changing) stars, since most, if not all their extra power around their main frequency components originates from phase/frequency change, although some contribution from amplitude change cannot be excluded.

If we consider the signs and sizes of the derived period change rates, we see that: (a) there are both positive and negative values; (b) in absolute values they are about two orders of magnitude larger than the ones expected from standard stellar evolution theory (e.g., Lee 1991). This type of discrepancy (although perhaps at a lower degree)

exists for most of the observed period changes in RR Lyrae stars. The explanation of this fact poses a serious challenge for stellar pulsation theory. Because the individual period changes are well-demonstrated and rather accurately measured, we think that it is incorrect to treat large period changes as errors and use only their averages over the variables studied (e.g., Lee 1991; Lee & Carney 1999; see however Rathbun & Smith 1997).

We list the RR1-*PC* variables found during this survey in Table 4. We caution that in some cases three prewhitenings with the main and two very close side components yield flat frequency spectra (e.g., 3.6240.470; 6.6568.484; 11.9235.1034). This suggest that these stars might turn out to be RR1-*BL* variables with very long modulation periods when future observations on a longer time base will be available.

7. MISCELLANEOUS VARIABLES

Either because of their rare occurrence or because of the specific frequency values of their secondary components, it is difficult to classify these stars with high confidence. Nevertheless, future studies might shed light both on the nature of these stars and on the possible relations between them and the more securely classified variables.

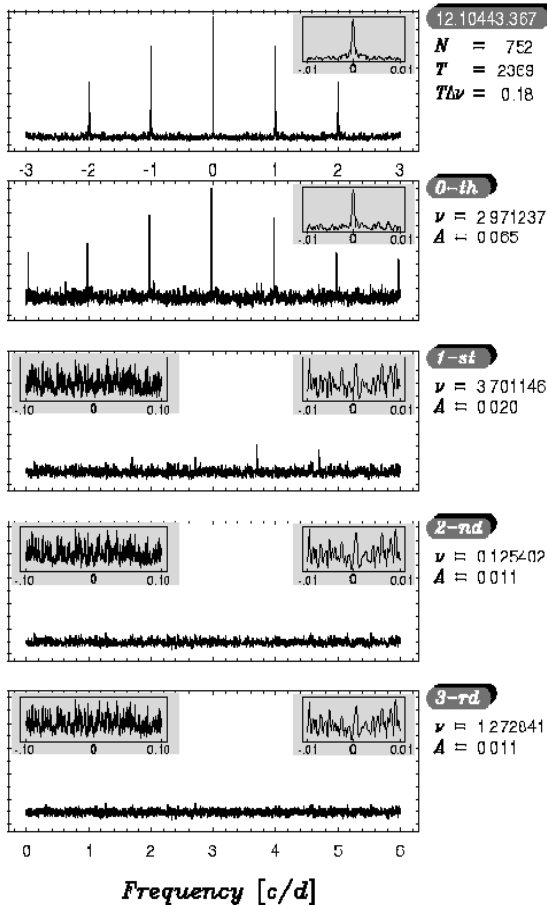


Fig. 19 – A suspected double-mode variable pulsating in the first and second overtones. For notation, see Figure 3.

There are 20 stars whose prewhitened frequency spectra contain residuals at integer d^{-1} components. Hereafter

we call these variables of RR1-*D1*-type. Usually, the amplitudes of these curious components are not too large, exceeding 50% of the main components only in two variables. For half of them this quantity is under 30%. In general, the secondary components show up at $1.00027 d^{-1}$ but sometimes the $\pm 1 d^{-1}$ aliases are stronger. As a result, it is possible that in some cases a long-term effect is responsible for the observed frequency pattern. We find many cases when the ‘b’ data do not justify the RR1-*D1* classification. For these variables we retain their RR1 status. Most probably, the RR1-*D1* variables are affected by some spurious observational or data reduction flaws, to be clarified in the future.

In three more interesting cases the frequency ratios of the secondary and main components closely resemble those of the first and second overtone modes of RR Lyrae models. Therefore, these preliminarily classified double-mode variables are referred to as RR12-type. One of them is shown in Figure 19. Further studies of these variables would be important for the verification of their double-mode behavior and their relations to the single-mode second overtone suspects (Alcock et al. 1996).

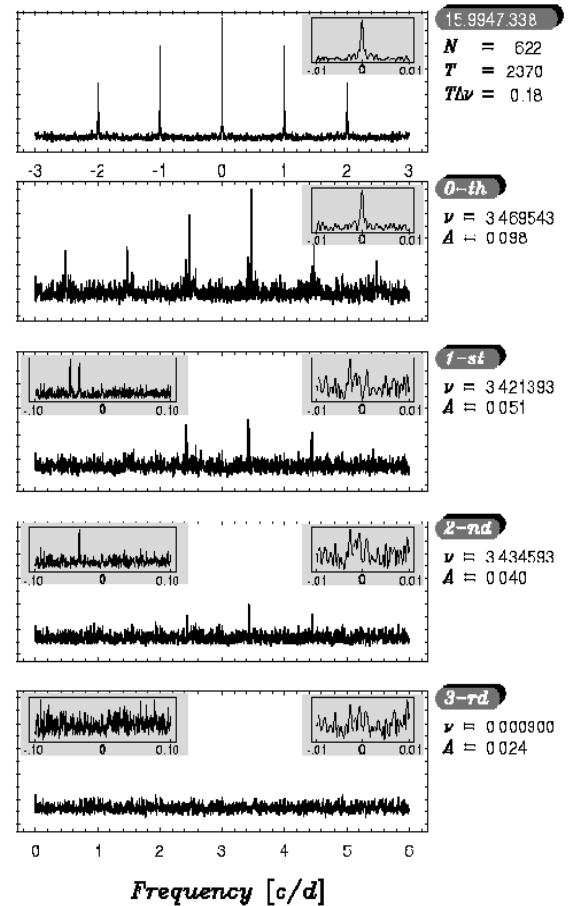


Fig. 20 – An example of the few RR1- ν 2-type variable found in the RR1 sample. For notation, see Figure 3.

In the frequency spectra of three variables we find two significant peaks close to the main component. However, unlike in the case of Blazhko stars, these peaks are *not spaced equidistantly*. We refer to these stars as

RR1- ν 2-type variables. Figure 20 displays the interesting case of 15.9947.338, where the two additional components are located close to each other, but further away from the main component. Another star, 2.5023.5787 shows three peaks of equal heights and asymmetric frequency spacing ($\delta f = 0.0030 \text{ d}^{-1}$). Because of the proximity of their frequency components, one may wonder whether the RR1- ν 1, RR1- ν 2- and Blazhko-type phenomena are physically related. At this moment it is not possible to deal with this question. Further detailed observational and theoretical works are needed.

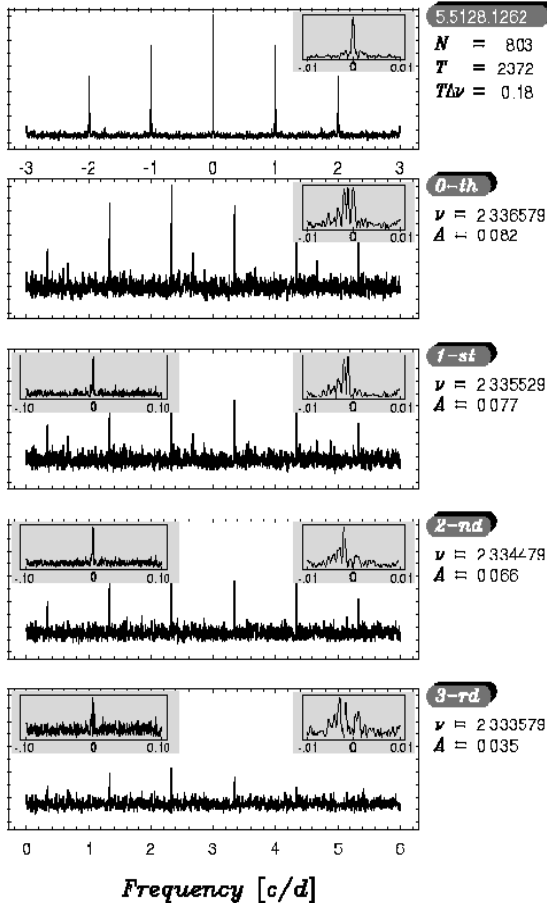


Fig. 21 – An example of the few RR1- ν M-type variable found in the RR1 sample. For notation, see Figure 3.

In five cases there are hints that the prewhitened spectra consist of several well-resolved peaks located close to the main component. Figure 21 displays the frequency spectra of one such variable. Following the nomenclature of the other variables with close components, we refer to these stars as RR1- ν M-type variables. It is tempting to identify these objects with multimode variables whose secondary frequency components correspond to some of the most strongly excited nonradial modes belonging to the same harmonic degree l (for recent theoretical models see Dziembowski, & Cassisi 1999). However, it is better to wait with this conclusion until more elaborated observational tests become available.

We also mention the relatively small group of variables whose classification is hampered by the complexity of their

spectra. This complexity is either due to the appearance of peaks without any hints of their origin, or to the high noise/low data number. These non-classified (RR1- NC) variables are listed together with Figure e above mentioned miscellaneous objects in Table 5. For further reference, in Table 6 we give the frequencies and amplitude ratios of the RR12 and RR1- ν 2 stars. The symbols ν_i refer to the frequencies obtained at the various stages of the prewhitening sequences, and not to the normal modes, within the system of standard notation for these modes.

It is important to recall that in some cases, in other types of variables described in the previous sections, we also encountered some peculiarities. First of all, because of the finite noise level and of the color dependence of the observed amplitudes, the ‘r’ and ‘b’ data sometimes yield inconsistent results. These situations occur usually when the secondary component is close to the noise level. In these cases classification is based on the ‘cleanest’ frequency spectrum. For RR1- D 1-type variables this practice is partially overruled by the fact that the secondary component is most probably an artifact, therefore, preference is given to the monophasic RR1 classification if it is supported by one of the colors. As another example for the possible ambiguity, we recall the case of some RR1- PC variables mentioned in Sect. 6. In the case of these stars the length of the available data is still too short to enable us to make a clear distinction between period change and the more than $\approx 2000 \text{ d}$ modulation period if the variable is of Blazhko-type, as it is suggested by the successive prewhitenings.

8. CONCLUSIONS

A massive frequency analysis has been carried out on a large sample of the first overtone RR Lyrae (RR1) population of the MACHO variable star base of the Large Magellanic Cloud. The study was aimed primarily at finding multiperiodic and non-stationary variables among RR1 stars. Special effort was made to search for amplitude- and phase-modulated (Blazhko) variables. Occurrence of this phenomenon among RR1 stars was not known previously. Because widely acceptable theoretical interpretation of the Blazhko effect is still missing, it is important to accumulate more observational data in order to constrain further the possible models. Because of the high occurrence rate of the Blazhko effect among fundamental mode RR Lyrae stars and the lack of theoretical understanding of this phenomenon, known for almost a century, further study of these stars has a general significance.

The basic technique of analysis we applied was the standard Fourier frequency analysis with the important sequential steps of prewhitening. All 1350 variables passed through a basic analysis which resulted in the selection of more than 400 multimode candidates for further studies. In Table 7 we summarize the statistics of the various types of variables we identified in the sample. This table does not contain the more than 30 doubly identified variables which were among the 1350 stars in the basic analysis of the data set. However, to make the statistics more complete, we added the 73 double-mode (RR01) variables of Alcock et al. (1997) to the newly discovered 108 stars of this study. As we have already warned in the paper, the classification of some of the variables may not be definitive. Although this results in some ambiguity in

TABLE 7
 VARIABLE TYPES IN THE MACHO DATABASE FOR THE FIRST OVERTONE RR LYRAE STARS IN THE LMC

<i>Type</i>	<i>Short description</i>	<i>Number</i>	<i>%</i>	<i>σ(%)</i>
RR1	Single-mode	916	69.0	1.3
RR1- ν 1	1 close component	24	1.8	0.4
RR1- ν 2	2 asymmetric close components	3	0.2	0.1
RR1- ν M	Multifrequency close components	5	0.4	0.2
RR1-BL	2 symmetric close components	28	2.1	0.4
RR1-PC	Period change	141	10.6	0.9
RR01	1st & 0th overtone double-mode	181	13.6	0.9
RR12	2nd & 1st overtone double-mode	3	0.2	0.1
RR1-D1	Integer d^{-1} frequencies	20	1.5	0.3
RR1-NC	Non-classified	6	0.5	0.2

NOTE.—The symbol σ (%) denotes the standard deviation of the population ratio, assuming Poisson distribution in the different populations.

the derived statistics, it does not change our basic conclusions. Furthermore, because of the finite noise level, there is a limit for the lowest detectable secondary signal components. Considering specifically the Blazhko-type stars, from the statistical tests presented in Sect. 5, we estimate this limit to be 10–15% in the units of the main signal component (10% being the level of marginal, whereas 15% is the level of close to secure detectability).

The 108 newly discovered RR01 stars follow the pattern on the $P_0 \rightarrow P_1/P_0$ diagram of the already known 73 double-mode variables (Alcock et al. 1997). This pattern implies metallicity and/or mass spread among the RR01 population of the LMC. Direct metallicity measurements through the ΔS method by Clementini et al. (2000) suggest the existence of sufficient [Fe/H] spread. The preliminary theoretical work of Popielski & Dziembowski (2000) comes to a similar conclusion. Accurate photometry and metallicity measurements of these stars would be very valuable also for constraining further the LMC distance scale (Kovács & Walker 1999).

We found three variables suspected for double-mode pulsations in the first and second overtones. Further study of these stars with additional photometry would be necessary to confirm their suggested pulsational status.

A considerable fraction of the RR1 population shows period change. Although some of them can be approximated by linear period changes, their high values exclude any evolution-related explanation. Understanding period changes in these and in other RR Lyrae stars remains an important unsolved problem in stellar pulsation theory.

We regard the most exciting finding of this study the discovery of the variables with closely spaced frequencies (for preliminary works on these and some fundamental mode Blazhko stars we refer to Kovács et al. 2000 and Kurtz et al. 2000). About half of these stars show only two components, similarly to the recent discoveries of the same type of stars by Olech et al. (1999a,b) and Moskalik (2000). Although in some of these RR1- ν 1-type stars

in our sample a weak third component with symmetric frequency spacing can be suspected, neither the large majority of our RR1- ν 1 stars, nor the variables reported by other authors show such components. However, in 28 variables we observe symmetric frequency spacing, very similar to the frequency spectra of the fundamental mode (RR0) Blazhko-type variables (e.g., Kovács 1995). Therefore, we associate these variables with the Blazhko-type stars. At this moment it is only the LMC in which first overtone Blazhko stars have been identified.

Compared with the commonly used incidence rate of 20–30% of the RR0 Blazhko variables (Szeidl 1988), our 2% frequency among RR1 stars seems to indicate that whatever is the underlying cause of the Blazhko phenomenon, it should work quite *differently* in RR1 than in RR0 stars. Although in a milder sense, this difference still survives even if we consider the recent statistics obtained by Moskalik (2000) on the OGLE sample of Galactic bulge RR Lyrae stars. He found 11 Blazhko variables from the 149 RR0 stars but none from the 66 RR1 stars analyzed (however, he found RR1- ν 1-type stars: 11 among the RR0, and 2 among the RR1 stars). According to our tests, if the lowest level of modulation among RR1 stars were 15%, assuming 20% incidence rate for the Blazhko phenomenon, we should have detected at least 30 more variables of this type. Although with a 10% modulation level under the same circumstance this number decreases to about 10, it is still large enough to conclude that we probably have not missed any Blazhko RR1 variables above the 10% modulation level. Adding to these that the high frequency of the Blazhko RR0 stars refers to relatively older data with marginal probability of the detection of low-amplitude modulations, and that most of them have 30–50% total modulation level, we think that the large difference in the occurrence rates of the two types of Blazhko stars is significant.

It follows from this result that *magnetic oblique rotator* model (Shibahashi 1994; 2000) of the Blazhko phe-

nomenon must face with the difficulty in explaining why the role of magnetic field becomes so much less important as a star pulsating in the fundamental mode and showing Blazhko phenomenon moves to the RR1 regime. Most of these stars must either stop being Blazhko-type variables, or their modulation level must decrease from 30–50% down to below 10% (in the units of the total pulsation amplitude). In addition, there is also the problem of asymmetric modulation amplitudes. This difficulty becomes extreme for the above theory to explain both Blazhko- and RR1– ν 1-type variables within the same framework. In order to deal with these basic observational facts, the magnetic model needs to be more complex than it is now. This, without the precise measurement of magnetic field, would lead to introducing more free parameters, and thereby to decreasing the predictive power of the theory.

The other theory, the model of *direct* ($\omega_0 \approx \omega_l$) *resonant mode coupling between a radial and nonradial modes* stays within the framework of nonlinear stellar pulsation, without invoking the presence of magnetic field. According to Van Hoolst, Dziembowski & Kawaler (1998), with significant probability this resonance is capable of destabilizing the fundamental limit cycle and leading either to steady *phase locked* pulsation, or to an amplitude- and phase-modulated one. In both cases we would see Blazhko variability but in the steady amplitude and phase solution observability would depend on the aspect angle of the observer relative to the rotation axis. Concerning the resonance theory, it is important to remark that the recent linear pulsation survey of Dziembowski & Cassisi (1999) shows that the excitation rates for the resonant $l = 1$ modes are comparable to those of the radial fundamental and first overtone modes. Although these results are encouraging, many questions remain to be answered, such as the relation between RR1– ν 1- and Blazhko-type stars,

and, of course, the low number of the Blazhko RR1 stars.

We look forward to completing a similar survey of multimode RR Lyrae stars in our six fields in the Small Magellanic Cloud. While we do not anticipate significant differences in the fractions of the types of multimode RR Lyrae variables or sample metallicity, such a survey will provide a test of the degree to which such samples are homogeneous. In many cases the signal-to-noise of the SMC RR Lyrae photometry is expected to be better than that of the LMC photometry because our SMC exposure times were twice as long and this more than compensates for the greater distance of the SMC.

This work was initiated during GK's stay at the IGPP of the Lawrence Livermore Laboratory. He thanks the director and the staff for their hospitality. Fruitful discussions with Hiromoto Shibahashi are very much appreciated. We thank Wojtek Dziembowski for his valuable comments as a referee. We are very grateful for the skilled support given our project by the technical staff at the Mt. Stromlo Observatory. Work performed at LLNL is supported by the DOE under contract W7405-ENG-48. Work performed by the Center for Particle Astrophysics on the UC campuses is supported in part by the Office of Science and Technology Centers of NSF under cooperative agreement AST-8809616. Work performed at MSSSO is supported by the Bilateral Science and Technology Program of the Australian Department of Industry, Technology and Regional Development. KG acknowledges a DOE OJI grant, and CWS and KG thank the Sloan Foundation for their support. DLW was a Natural Sciences and Engineering Research Council (NSERC) University Research Fellow during this work. DM is supported by Fondecyt 1990440. The supports of the following grants are acknowledged: OTKA T-024022, T-026031 and T-030954.

REFERENCES

- Alcock, C. & the MACHO collaboration. 1996, AJ, 111, 1146
 Alcock, C. & the MACHO collaboration. 1997, ApJ, 482, 89 (A97)
 Alcock, C. & the MACHO collaboration. 1999, PASP, 111, 1539
 Borkowski, K. J. 1980, Acta Astr., 30, 393
 Clementini, G., Bragaglia, A. Carretta, E. & Di Fabrizio, L. 2000, ASP Conf. Ser., 203, 172
 Cox, A. N., Hodson, S. W., & Clancy, S. P. 1983, ApJ, 266, 94
 Deeming, T. J. 1975, Ap&SS, 36, 137
 Dziembowski, W. A. & Cassisi, S. 1999, Acta. Astr., 49, 371
 Goranskij, V. P. 1981, Inf. Bull. Variable Stars, 2007
 Jerzykiewicz, M & Wenzel, W. 1977, Acta Astr., 27, 35
 Kovács, G. 1995, A&A, 295, 693
 Kovács, G., Buchler, J. R. & Marom, A. 1991, A&A, 252, L27
 Kovács, G. & Walker, A. R. 1999, ApJ, 512, 271
 Kovács, G. & the MACHO Collaboration. 2000, ASP Conf. Ser., 203, 313
 Kurtz, D. W. & the MACHO Collaboration. 2000, ASP Conf. Ser., 203, 291
 Lee, J.-W. & Carney, B. W. 1999, AJ, 117, 2868
 Lee, Y.-W. 1991, ApJ, 367, 524
 Moskalik, P. 2000, ASP Conf. Ser., 203, 315 (M00)
 Nagy, A. 1998, A&A, 339, 440
 Olech, A., Kałużny, J., Thompson, I., Pych, W., Krzemiński, W. & Schwarzenberg-Czerny, A. 1999a, AJ, 118, 442 (O99a)
 Olech, A., Woźniak, P. R., Alard, C. Kaluzny, J. & Thompson, I. B. 1999b, *Month. Not. Roy. Astr. Soc.*, astro-ph 9905065. (O99b)
 Petersen, J. O. 1973, A&A, 27, 89
 Popielski, B. L. & Dziembowski, W. A. 2000, ASP Conf. Ser., 203, 276
 Rathbun, P. G. & Smith, H. A. 1997, PASP, 109, 1128
 Sandage, A., Katem, B. & Sandage, M. 1981, ApJS, 46, 41
 Shibahashi, H. 1994, ASP Conf. Ser., Vol. 76, 618
 Shibahashi, H. 2000, ASP Conf. Ser., 203, 299
 Smith, H. A., Matthews, J. M., Lee, K. M., Williams, J., Silbermann, N. A. & Bolte, M. 1994, AJ, 107, 679
 Smith, H. A., Barnett, M., Silbermann, N. A. & Gay, P. 1999, AJ, 118, 572
 Szeidl, B. 1988, in *Multimode Stellar Pulsations*, Kultúra, Konkoly Observatory, Budapest; Eds.: G. Kovács, L. Szabados and B. Szeidl, p. 45.
 Szeidl, B. & Kolláth, Z. 2000, ASP Conf. Ser., 203, 281
 Udalski, A. Soszyński, I., Szymański, M., Kubiak, M., Pietrzyński, G., Woźniak, P. and Żebruń, K. 1999, Acta Astr., 49, 1
 Van Hoolst, T., Dziembowski, W. A. & Kawaler, S. 1998, MNRAS, 297, 536

TABLE 1
PREVIOUSLY NOT KNOWN RR01 VARIABLES OF THE MACHO RR1 SAMPLE

MACHO #	α	δ	P_1	P_1/P_0	A_1	A_0/A_1
80.7193.1485	05:24:39.0	-69:20:27	0.328818	0.7419	0.163	0.319
81.8639.1450	05:33:27.0	-69:42:19	0.335257	0.7415	0.091	0.396
10.4043.1392	05:05:43.3	-69:34:13	0.343077	0.7427	0.128	1.078
80.7439.1836	05:26:14.5	-69:03:33	0.343358	0.7429	0.136	1.184
5.4889.1102	05:10:35.6	-69:39:11	0.343666	0.7427	0.108	1.009
14.9220.799	05:37:10.7	-71:21:15	0.343895	0.7433	0.152	0.704
5.5254.1692	05:12:57.8	-69:33:39	0.345360	0.7430	0.112	0.384
5.4524.1212	05:08:13.5	-69:46:46	0.346200	0.7435	0.152	0.322
14.9467.864	05:38:53.0	-71:00:13	0.346562	0.7437	0.116	0.362
80.7073.1658	05:24:00.3	-69:15:00	0.347832	0.7433	0.141	0.823
6.6086.792	05:17:59.1	-70:30:25	0.348080	0.7438	0.128	0.344
82.8410.986	05:32:28.1	-68:52:04	0.348386	0.7432	0.142	0.563
3.7448.428	05:26:20.0	-68:28:54	0.348508	0.7429	0.123	0.382
15.10797.871	05:46:46.9	-71:03:52	0.348567	0.7430	0.134	0.701
3.7447.739	05:25:54.5	-68:29:42	0.349064	0.7437	0.126	0.286
81.8882.1067	05:34:51.2	-69:41:06	0.349122	0.7431	0.101	0.851
6.6214.4637	05:18:57.3	-70:02:04	0.349177	0.7432	0.086	0.930
81.9118.1794	05:36:42.8	-70:05:01	0.350143	0.7432	0.148	0.939
2.4904.1651	05:10:20.5	-68:39:40	0.350355	0.7437	0.126	0.635
9.5487.736	05:13:58.4	-70:09:06	0.350612	0.7436	0.123	0.447
18.2717.812	04:56:51.9	-69:16:01	0.350658	0.7440	0.116	0.586
80.6590.1844	05:21:07.3	-69:11:15	0.351176	0.7437	0.122	0.615
9.4873.519	05:10:50.7	-70:42:24	0.351258	0.7438	0.127	0.843
14.9587.828	05:39:21.7	-71:01:47	0.351263	0.7433	0.134	0.567
15.10071.888	05:42:25.3	-71:02:45	0.352199	0.7439	0.116	0.957
14.9703.450	05:40:11.9	-71:23:48	0.352214	0.7440	0.129	0.271
11.9838.1201	05:40:46.4	-70:26:21	0.352312	0.7442	0.149	0.215
6.5732.3906	05:15:56.2	-69:57:23	0.352354	0.7437	0.097	0.907
15.10071.765	05:42:44.5	-71:04:15	0.352895	0.7442	0.138	0.558
9.4275.536	05:07:13.3	-70:17:38	0.353072	0.7437	0.131	0.832
9.5124.1174	05:11:43.8	-70:08:09	0.353582	0.7439	0.148	0.669
18.2234.1176	04:54:36.2	-69:13:03	0.353711	0.7440	0.152	0.658
82.8169.654	05:30:44.5	-68:47:50	0.353998	0.7442	0.112	0.509
6.6452.704	05:20:00.6	-70:20:44	0.354096	0.7438	0.135	0.800
2.5274.1185	05:12:28.3	-68:09:49	0.355067	0.7438	0.129	0.465
6.5730.3869	05:15:48.4	-70:02:35	0.355162	0.7442	0.103	0.456
6.5853.3986	05:16:26.5	-69:57:38	0.355413	0.7436	0.141	0.248
3.7331.467	05:25:43.5	-68:11:51	0.355927	0.7441	0.137	0.723
19.3581.468	05:02:32.6	-68:08:06	0.356444	0.7440	0.140	0.750
9.5119.644	05:12:09.8	-70:28:05	0.356593	0.7437	0.123	0.626
13.6925.627	05:23:35.0	-71:03:46	0.356680	0.7442	0.125	0.440
3.6725.519	05:22:02.1	-68:16:24	0.356781	0.7441	0.139	0.410
82.8886.1146	05:35:21.4	-69:23:09	0.357001	0.7445	0.142	0.577
80.7202.4678	05:24:29.6	-68:45:33	0.357115	0.7442	0.121	0.430
80.7071.5289	05:23:52.4	-69:25:22	0.357209	0.7441	0.162	0.673
13.6197.522	05:18:58.1	-71:11:37	0.357237	0.7442	0.149	0.342
3.7082.957	05:23:52.3	-68:41:00	0.357462	0.7436	0.113	0.664
9.4514.979	05:08:30.1	-70:27:36	0.357478	0.7446	0.144	0.257
11.8750.1694	05:34:14.2	-70:25:18	0.357774	0.7438	0.139	0.856
3.6963.574	05:23:34.4	-68:30:28	0.358068	0.7447	0.131	0.603
19.4429.703	05:07:45.6	-68:03:35	0.358129	0.7446	0.137	0.350
5.4892.3500	05:10:54.2	-69:28:24	0.358174	0.7444	0.165	0.382
19.4308.880	05:06:45.6	-68:03:25	0.358336	0.7444	0.132	0.409
6.6574.1353	05:20:45.0	-70:14:38	0.358535	0.7444	0.149	0.289
19.3702.545	05:03:24.2	-68:08:53	0.358756	0.7436	0.068	0.603
19.4057.1115	05:05:39.6	-68:40:34	0.358970	0.7443	0.130	0.231
10.4522.4058	05:08:25.8	-69:56:21	0.358983	0.7446	0.129	0.589
6.6089.1661	05:17:44.5	-70:19:27	0.359199	0.7442	0.151	0.662
10.4035.1299	05:05:11.2	-70:08:25	0.359503	0.7440	0.132	0.702
6.6329.884	05:19:16.2	-70:26:40	0.359788	0.7431	0.134	0.269
82.8889.452	05:35:01.6	-69:13:24	0.360186	0.7445	0.073	0.658
6.6212.1063	05:18:32.7	-70:12:21	0.360280	0.7445	0.105	0.514
13.5842.2316	05:16:27.6	-70:38:57	0.360422	0.7451	0.140	0.664
80.7072.2154	05:24:05.6	-69:21:13	0.360853	0.7443	0.165	0.400
11.9595.1162	05:39:39.1	-70:30:27	0.361067	0.7429	0.090	1.056
19.4541.1357	05:08:42.6	-68:40:30	0.361879	0.7436	0.128	0.938
11.8985.882	05:35:44.3	-70:53:11	0.362499	0.7443	0.132	0.765
5.4767.962	05:09:56.7	-69:42:31	0.363025	0.7439	0.139	0.331
13.6927.606	05:23:22.7	-70:57:02	0.363183	0.7450	0.133	0.195
82.7922.520	05:29:13.8	-69:08:28	0.363555	0.7446	0.106	0.796
12.10682.793	05:40:27.0	-70:39:00	0.363690	0.7441	0.110	0.373
2.5389.1138	05:13:38.8	-68:36:13	0.364125	0.7452	0.124	0.444
15.10557.2954	05:45:15.9	-70:54:36	0.364422	0.7444	0.130	0.623
3.7208.477	05:24:24.6	-68:21:09	0.364541	0.7451	0.139	0.504
9.5238.804	05:13:02.4	-70:36:07	0.365550	0.7450	0.150	0.300
47.2619.1486	04:56:32.8	-67:44:22	0.365873	0.7443	0.102	0.912
9.4881.635	05:10:52.4	-70:12:50	0.366304	0.7446	0.104	0.673
12.11172.776	05:49:17.8	-70:16:26	0.366906	0.7451	0.118	0.636
9.5483.1857	05:14:21.3	-70:21:47	0.367222	0.7444	0.160	0.569
10.3798.927	05:04:07.1	-69:47:41	0.367266	0.7443	0.102	1.000
12.10679.968	05:45:56.5	-70:50:38	0.367586	0.7447	0.161	0.565
14.8982.1963	05:36:05.0	-71:01:56	0.367633	0.7448	0.120	0.633
80.6830.2303	05:22:15.9	-69:20:43	0.367640	0.7446	0.125	0.608
18.2601.439	04:56:30.3	-68:54:44	0.367645	0.7444	0.124	0.927
80.7072.1233	05:23:47.3	-69:18:19	0.367710	0.7456	0.126	0.429
82.8163.1039	05:30:30.4	-69:12:46	0.367774	0.7447	0.142	0.655
5.5136.5295	05:11:44.3	-69:21:40	0.367867	0.7442	0.105	0.705
80.7313.4672	05:25:34.2	-69:24:16	0.368165	0.7446	0.147	0.741
12.9962.1419	05:41:49.1	-70:16:24	0.368761	0.7443	0.147	0.571
13.6804.494	05:22:21.3	-71:05:07	0.369552	0.7449	0.126	0.429
10.4042.1202	05:05:24.3	-69:40:04	0.370325	0.7444	0.137	0.584
80.7321.1365	05:25:16.5	-68:52:07	0.370618	0.7442	0.131	0.817
9.5358.566	05:13:39.0	-70:41:20	0.371015	0.7450	0.127	0.661
6.5850.933	05:16:15.4	-70:08:14	0.373065	0.7447	0.102	0.784
5.5247.894	05:12:15.9	-69:57:54	0.373214	0.7447	0.118	0.805
6.6572.919	05:21:16.6	-70:22:03	0.375591	0.7448	0.111	0.514
6.5721.352	05:16:05.9	-70:39:36	0.376642	0.7460	0.116	0.586
2.4789.1029	05:09:57.6	-68:17:04	0.382408	0.7461	0.132	0.326
5.5369.1184	05:13:39.0	-69:54:23	0.383798	0.7457	0.129	0.605
47.2247.648	04:54:06.1	-68:19:46	0.392076	0.7448	0.135	0.607
10.3557.827	05:02:18.2	-69:42:31	0.393324	0.7455	0.123	0.537
11.9231.545	05:37:10.7	-70:37:11	0.393474	0.7461	0.089	0.472
5.5492.1293	05:13:57.2	-69:47:06	0.394394	0.7461	0.142	0.493
10.4041.840	05:05:33.2	-69:45:00	0.398820	0.7461	0.117	0.504
19.4182.345	05:06:27.0	-68:24:43	0.401265	0.7457	0.129	0.364
10.3191.363	05:00:53.5	-69:55:49	0.406071	0.7450	0.102	0.591
11.8867.861	05:35:25.9	-70:41:31	0.413194	0.7465	0.128	0.312
19.4785.5170	05:09:47.1	-68:33:13	0.428630	0.7458	0.112	0.259

TABLE 2
RR1- ν 1 VARIABLES OF THE MACHO RR1 SAMPLE

<i>MACHO #</i>	α	δ	ν_0	A_0	$\nu_1 - \nu_0$	A_1/A_0
47.2609.56	04:56:45.1	-68:21:41	2.79858	0.112	-0.01421	0.268
14.9225.776	05:37:19.7	-70:59:08	2.81588	0.174	-0.05414	0.241
6.6326.424	05:19:30.1	-70:39:32	3.02616	0.169	-0.07267	0.195
6.6091.877	05:18:01.8	-70:11:47	3.11905	0.062	-0.03855	0.694
13.5714.442	05:15:29.3	-71:08:09	3.15586	0.067	0.10922	0.716
80.6352.1495	05:19:37.7	-68:56:37	3.24687	0.070	-0.07175	0.671
13.6204.617	05:18:41.2	-70:43:53	3.41120	0.107	-0.05116	0.271
15.10072.918	05:42:11.3	-70:58:22	3.41207	0.195	-0.03687	0.210
10.3552.745	05:02:37.6	-70:03:31	3.42121	0.072	0.03745	0.611
5.5489.1397	05:14:36.8	-69:58:30	3.44866	0.143	-0.04786	0.350
10.4161.1053	05:06:14.6	-69:47:06	3.47877	0.100	0.09394	0.380
15.11036.255	05:48:09.0	-71:17:19	3.48510	0.070	0.07820	0.829
11.9471.780	05:38:33.6	-70:43:58	3.49672	0.160	-0.11346	0.275
9.5242.1032	05:12:43.9	-70:20:02	3.49779	0.126	0.03749	0.563
13.5713.590	05:15:25.7	-71:10:31	3.52566	0.076	0.10042	0.553
82.8289.887	05:31:19.2	-68:50:33	3.53404	0.103	-0.18970	0.311
2.5266.3864	05:12:36.8	-68:43:38	3.57930	0.127	0.06554	0.370
80.7072.2280	05:23:45.4	-69:20:54	3.58891	0.105	-0.04727	0.257
80.7437.1678	05:26:25.3	-69:12:11	3.59531	0.128	-0.08894	0.688
6.5729.958	05:16:01.3	-70:06:44	3.59948	0.117	0.07423	0.761
3.6603.795	05:20:41.0	-68:20:21	3.61654	0.179	-0.01735	0.218
6.5730.4057	05:16:02.0	-70:05:10	3.61898	0.077	0.07758	0.636
14.9702.401	05:40:17.6	-71:26:48	3.63103	0.163	-0.18408	0.196
82.8766.1305	05:34:23.3	-69:20:04	3.85726	0.080	-0.00306	0.550

NOTE.—

13.6204.617 – ‘b’ data support RR1 status

47.2609.56 – also an RR01 variable with $P_1/P_0 = 0.7443$ and $A_1/A_0 = 0.22$

6.5729.958 – in ‘b’ there is a third component at $P(\nu_2)/P(\nu_0) = 0.757$

82.8766.1305 – hint for RR1-*BL* classification in the ‘b’ data

TABLE 3
RR1–BL VARIABLES OF THE MACHO RR1 SAMPLE

<i>MACHO #</i>	α	δ	f_0	A_0	Δf_- Δf_+	A_-/A_0 A_+/A_0
81.8758.1447	05:34:39.1	-69:51:33	2.19180	0.283	-0.02987 0.02991	0.117 0.170
6.7054.713	05:24:03.1	-70:33:38	2.27063	0.152	-0.00166 0.00163	0.224 0.132
2.5271.255	05:13:05.0	-68:22:49	2.30017	0.113	-0.00129 0.00121	0.345 0.469
80.6957.409	05:23:27.6	-68:55:38	2.45168	0.104	-0.00084 0.00079	0.183 0.298
3.6240.450	05:19:03.1	-68:20:21	2.60663	0.155	-0.00099 0.00104	0.258 0.271
81.8639.1749	05:33:52.6	-69:43:21	2.66022	0.135	-0.04469 0.04482	0.200 0.252
19.4188.1264	05:06:01.5	-68:00:45	2.70082	0.127	-0.00096 0.00105	0.402 0.591
80.6953.1751	05:23:31.4	-69:11:07	2.84322	0.182	-0.02811 0.02808	0.280 0.341
15.10311.782	05:44:00.5	-71:10:42	2.87117	0.146	-0.00106 0.00118	0.240 0.226
5.5368.1201	05:13:44.2	-70:00:45	2.97166	0.197	-0.00558 0.00552	0.264 0.137
80.6595.1599	05:21:08.3	-68:51:17	3.00869	0.128	-0.03684 0.03683	0.484 0.250
18.2361.870	04:54:43.2	-68:48:06	3.07240	0.137	-0.02973 0.02974	0.263 0.358
82.8526.1176	05:32:47.6	-69:11:52	3.08750	0.066	-0.12705 0.12704	0.288 0.227
9.5479.852	05:14:08.3	-70:39:32	3.10820	0.154	-0.00069 0.00078	0.532 0.675
14.9223.737	05:37:36.3	-71:06:35	3.22706	0.148	-0.03161 0.03159	0.439 0.486
82.8765.1250	05:34:02.0	-69:21:56	3.27951	0.159	-0.04898 0.04900	0.252 0.264
82.8049.746	05:29:34.8	-68:45:34	3.34744	0.162	-0.07194 0.07191	0.278 0.247
15.10068.239	05:42:11.3	-71:14:50	3.35914	0.124	-0.03338 0.03351	0.274 0.177
82.8408.1002	05:32:00.7	-68:58:50	3.37504	0.163	-0.03544 0.03542	0.221 0.325
2.5148.1207	05:12:23.9	-68:29:43	3.39346	0.121	-0.03528 0.03526	0.289 0.273
15.10313.606	05:43:45.0	-71:04:54	3.41874	0.128	-0.06431 0.06438	0.422 0.477
13.6810.2992	05:22:45.6	-70:39:11	3.44356	0.125	-0.04147 0.04159	0.664 0.456
6.5971.1233	05:16:59.0	-70:08:14	3.47563	0.120	-0.07350 0.07351	0.350 0.175
19.4188.195	05:06:26.3	-67:58:57	3.53583	0.123	-0.01215 0.01210	0.358 0.431
80.7441.933	05:26:06.4	-68:56:02	3.65881	0.130	-0.04795 0.04800	0.246 0.338
11.9355.1380	05:38:21.3	-70:23:22	3.70248	0.039	-0.00465 0.00466	2.308 1.333
5.4401.1018	05:07:33.5	-69:55:12	3.72395	0.076	-0.00480 0.00470	0.816 0.579
9.5125.1018	05:11:47.0	-70:05:37	3.84901	0.108	-0.00520 0.00519	0.500 0.204

NOTE.—
5.5368.1201 – ‘b’ data are used
9.5479.852 – ‘b’ data are used

TABLE 4
RR1-PC VARIABLES OF THE MACHO RR1 SAMPLE

<i>MACHO #</i>	α	δ	P_1	<i>MACHO #</i>	α	δ	P_1
2.5389.1478	05:13:40.9	-68:37:18	0.250558	3.6362.689	05:19:32.1	-68:16:48	0.357375
3.7450.214	05:26:25.7	-68:19:52	0.281339	18.2597.765	04:56:08.5	-69:12:11	0.357969
6.6094.5406	05:18:07.1	-70:00:05	0.285164	80.6838.2884	05:22:18.3	-68:46:38	0.358339
6.6810.616	05:22:16.7	-70:39:50	0.288385	80.7072.1545	05:23:45.0	-69:20:51	0.358344
14.8497.534	05:32:39.9	-71:07:44	0.289300	9.4873.497	05:10:45.8	-70:44:40	0.358621
13.6326.1733	05:19:49.9	-70:38:49	0.290353	6.5848.1122	05:16:14.7	-70:17:33	0.359143
13.6077.638	05:18:11.5	-71:08:05	0.290690	14.9590.3902	05:39:26.8	-70:50:32	0.360039
9.4394.386	05:07:58.5	-70:21:54	0.290778	5.4766.918	05:10:02.5	-69:46:33	0.361072
10.3557.1024	05:02:42.7	-69:43:47	0.294767	2.5872.1272	05:16:21.1	-68:37:57	0.362671
10.3556.986	05:02:04.4	-69:48:28	0.296149	9.5363.899	05:13:34.6	-70:21:08	0.364048
81.8879.1869	05:34:52.9	-69:51:52	0.297565	12.10801.843	05:47:04.2	-70:49:30	0.365089
80.7319.1287	05:25:31.4	-69:01:20	0.297860	13.6198.531	05:18:47.6	-71:05:58	0.366172
9.5599.762	05:15:17.5	-70:44:55	0.299416	9.4994.491	05:11:22.0	-70:44:24	0.366418
9.4760.861	05:09:36.4	-70:13:23	0.299667	11.9113.1731	05:36:38.0	-70:23:21	0.366441
12.10808.830	05:47:01.6	-70:18:09	0.300015	15.10914.663	05:47:22.6	-71:20:57	0.367050
9.4761.1258	05:09:58.6	-70:08:13	0.300939	10.4040.917	05:05:14.1	-69:47:53	0.367383
11.9116.1382	05:36:19.9	-70:13:36	0.302487	3.6598.939	05:21:03.0	-68:38:22	0.367820
80.7436.1463	05:26:04.6	-69:16:12	0.302509	3.6723.769	05:21:22.8	-68:23:46	0.369235
9.4392.833	05:07:35.7	-70:30:51	0.303440	82.8283.1040	05:31:19.5	-69:17:37	0.370077
18.3086.1308	04:59:08.1	-68:53:28	0.304942	13.5844.3963	05:16:10.1	-70:32:08	0.370272
15.10795.916	05:47:00.0	-71:11:37	0.307457	6.6212.1142	05:19:04.2	-70:11:59	0.373232
5.4767.1388	05:09:50.0	-69:44:26	0.307806	82.8406.1180	05:31:50.3	-69:08:37	0.373883
80.6597.4435	05:20:39.1	-68:45:14	0.308645	82.8288.869	05:31:02.9	-68:55:13	0.374056
10.3797.865	05:03:46.3	-69:53:20	0.308792	5.4524.972	05:08:42.3	-69:45:56	0.374232
80.7195.1166	05:25:01.1	-69:11:08	0.310755	13.6080.541	05:18:10.1	-70:57:30	0.374479
80.6951.2395	05:23:23.6	-69:18:38	0.311420	15.10069.680	05:42:26.9	-71:13:33	0.374508
19.4669.2905	05:09:21.0	-68:10:27	0.311959	2.4908.826	05:10:57.3	-68:22:22	0.376579
2.5630.1156	05:15:02.5	-68:39:15	0.312314	5.5008.1902	05:11:22.8	-69:48:30	0.377428
2.5151.924	05:12:06.2	-68:18:42	0.314624	19.4429.678	05:07:36.8	-68:02:37	0.377518
2.5514.660	05:14:27.9	-68:18:54	0.315373	5.4769.1363	05:10:01.1	-69:34:38	0.378528
3.7444.782	05:26:23.2	-68:44:13	0.317451	11.9355.1235	05:38:25.6	-70:23:42	0.379060
81.9004.1177	05:35:57.0	-69:33:52	0.318030	12.11042.810	05:48:12.8	-70:51:37	0.379823
9.4875.697	05:10:45.0	-70:35:11	0.320646	3.7205.727	05:24:30.4	-68:31:31	0.381238
2.5148.713	05:11:42.8	-68:32:12	0.321252	6.6813.699	05:22:13.9	-70:28:34	0.382572
5.4891.1617	05:10:26.3	-69:33:27	0.321780	6.5724.620	05:15:58.0	-70:28:48	0.382936
13.5721.2180	05:16:02.7	-70:39:39	0.322156	81.9123.806	05:36:40.7	-69:43:09	0.385314
11.9594.880	05:39:42.8	-70:37:17	0.322277	12.10924.961	05:47:58.7	-70:38:07	0.386863
6.6933.1043	05:23:22.3	-70:32:35	0.322842	2.5388.1150	05:13:35.5	-68:39:42	0.388582
3.7088.623	05:24:15.8	-68:16:34	0.324418	81.9723.894	05:40:15.9	-70:02:56	0.388602
82.8282.1019	05:31:08.0	-69:18:29	0.327110	5.5489.1125	05:14:33.3	-70:01:07	0.389857
80.7436.1633	05:26:10.9	-69:14:48	0.330471	80.6350.3508	05:19:37.6	-69:05:23	0.390063
9.5600.566	05:15:04.5	-70:41:39	0.331331	2.5876.444	05:16:27.5	-68:25:14	0.396680
5.4766.1109	05:09:48.8	-69:48:47	0.332465	6.6697.1361	05:21:35.2	-70:09:35	0.397333
6.6452.2394	05:20:25.3	-70:17:55	0.334832	9.4634.863	05:08:45.1	-70:33:10	0.398111
3.6240.470	05:19:06.4	-68:20:54	0.334995	9.4879.502	05:10:49.5	-70:18:28	0.398205
6.6455.1326	05:20:23.8	-70:09:14	0.335632	9.5364.886	05:13:45.4	-70:16:26	0.398766
6.6094.5331	05:18:17.8	-70:00:14	0.335685	13.6080.628	05:18:18.5	-70:55:58	0.400474
2.4787.770	05:10:11.9	-68:22:56	0.335706	6.5971.1194	05:17:36.9	-70:08:26	0.400978
81.9723.796	05:40:19.4	-70:05:40	0.336952	6.6451.919	05:20:22.7	-70:24:56	0.402077
19.3823.546	05:03:43.2	-68:06:29	0.337930	13.6441.529	05:20:19.2	-71:05:14	0.402531
13.6568.3005	05:20:42.8	-70:38:46	0.338099	11.9349.558	05:37:49.0	-70:47:36	0.402859
80.6950.6414	05:23:35.5	-69:21:54	0.338445	13.6080.594	05:18:18.0	-70:56:08	0.404710
6.6094.5606	05:18:13.2	-69:58:41	0.339385	81.8875.2038	05:34:57.0	-70:05:56	0.405794
15.10433.787	05:44:52.1	-71:06:48	0.339489	80.7192.3592	05:25:02.3	-69:24:50	0.405959
80.7440.1192	05:26:28.6	-68:59:17	0.343025	80.6953.1590	05:23:23.6	-69:10:17	0.406129
14.9346.412	05:38:13.8	-70:58:07	0.343495	82.8041.1029	05:30:00.7	-69:16:53	0.406715
13.6441.527	05:20:08.9	-71:05:36	0.343520	19.3823.473	05:03:42.4	-68:07:30	0.408980
80.6468.2765	05:20:30.5	-69:13:45	0.349369	81.8518.1621	05:33:02.9	-69:42:37	0.410623
6.5729.1008	05:15:47.5	-70:06:08	0.350106	9.4390.560	05:07:17.6	-70:38:15	0.411036
80.6835.1220	05:22:30.0	-68:57:42	0.350229	9.5360.903	05:13:29.3	-70:31:35	0.413897
10.4165.348	05:06:01.3	-69:32:29	0.350558	11.8744.658	05:34:10.4	-70:48:10	0.415590
19.4784.5754	05:09:51.5	-68:34:28	0.351798	14.8744.3716	05:34:10.6	-70:48:13	0.415694
2.5870.4598	05:16:38.9	-68:49:28	0.352372	11.9235.1034	05:37:13.5	-70:18:43	0.417598
15.10308.620	05:43:55.6	-71:23:39	0.353552	2.5273.1267	05:12:28.9	-68:16:07	0.420892
81.9724.295	05:40:22.2	-69:59:22	0.353864	13.6076.306	05:18:15.4	-71:13:35	0.427092
11.9471.1050	05:38:43.5	-70:42:47	0.354204	3.6236.690	05:18:36.8	-68:36:38	0.435675
3.6360.656	05:19:11.9	-68:23:37	0.354548	13.6926.490	05:22:56.2	-71:00:12	0.438382
6.6812.923	05:22:26.5	-70:30:19	0.354785	2.5271.1540	05:12:27.7	-68:25:31	0.439438
5.5250.1501	05:13:09.0	-69:46:38	0.355176	82.8890.449	05:34:44.2	-69:08:29	0.440049
2.4663.944	05:09:04.9	-68:34:50	0.355264	11.8867.970	05:35:14.5	-70:39:11	0.446641
6.6692.937	05:21:29.1	-70:29:23	0.356880				

TABLE 5
MISCELLANEOUS VARIABLES OF THE MACHO RR1 SAMPLE

<i>MACHO #</i>	α	δ	P_1	<i>Type</i>
9.4278.179	05:07:03.5	-70:04:06	0.326816	RR12
12.10443.367	05:44:36.9	-70:28:50	0.336559	RR12
12.10202.285	05:43:04.3	-70:22:47	0.398114	RR12
15.9947.338	05:41:43.0	-71:14:05	0.288221	RR1- ν 2
11.8987.787	05:36:05.9	-70:44:43	0.304127	RR1- ν 2
2.5023.5787	05:11:27.9	-68:47:50	0.324536	RR1- ν 2
14.8376.548	05:32:15.3	-71:08:10	0.291571	RR1- ν M
11.8751.1740	05:34:39.9	-70:20:55	0.357751	RR1- ν M
19.4671.684	05:09:14.5	-68:05:30	0.378744	RR1- ν M
5.5128.1262	05:11:43.2	-69:50:57	0.427975	RR1- ν M
6.6697.1565	05:21:49.6	-70:06:58	0.433493	RR1- ν M
12.11043.1000	05:48:19.1	-70:46:08	0.264320	RR1-NC
9.5123.633	05:11:45.6	-70:12:17	0.267730	RR1-NC
82.8525.1980	05:32:52.3	-69:13:51	0.283398	RR1-NC
9.5239.1141	05:12:44.3	-70:31:21	0.363336	RR1-NC
13.6802.544	05:22:43.5	-71:10:48	0.378060	RR1-NC
10.4403.4871	05:07:21.4	-69:46:46	0.457304	RR1-NC
6.6093.5030	05:18:05.1	-70:03:56	0.265360	RR1-D1
3.6243.404	05:18:42.4	-68:06:50	0.270851	RR1-D1
80.6353.1458	05:19:36.8	-68:49:41	0.275324	RR1-D1
9.5599.617	05:14:52.0	-70:45:24	0.278206	RR1-D1
80.6708.6771	05:21:27.0	-69:23:22	0.286094	RR1-D1
6.6815.747	05:22:31.1	-70:21:39	0.292024	RR1-D1
9.5004.750	05:11:36.8	-70:04:57	0.304161	RR1-D1
81.8521.1454	05:33:13.2	-69:31:35	0.309440	RR1-D1
3.6961.824	05:22:55.7	-68:39:54	0.309894	RR1-D1
9.5122.363	05:11:47.5	-70:16:17	0.322232	RR1-D1
6.6931.649	05:23:01.5	-70:39:45	0.322806	RR1-D1
12.10920.615	05:47:43.4	-70:54:12	0.323981	RR1-D1
5.4649.1029	05:09:08.2	-69:30:52	0.325266	RR1-D1
13.6806.664	05:22:17.6	-70:54:28	0.330759	RR1-D1
80.6709.2322	05:21:37.9	-69:21:26	0.332538	RR1-D1
9.5360.768	05:13:34.5	-70:29:57	0.337518	RR1-D1
14.8854.199	05:34:55.9	-71:29:44	0.339066	RR1-D1
81.8519.1395	05:32:48.6	-69:41:06	0.339398	RR1-D1
12.11283.284	05:49:38.5	-70:55:33	0.340384	RR1-D1
6.6699.5598	05:21:34.6	-70:01:18	0.352686	RR1-D1

TABLE 6
RR12 AND RR1- ν 2 VARIABLES OF THE MACHO RR1 SAMPLE

<i>MACHO #</i>	ν_0	ν_1	ν_2	ν_0/ν_1	A_1/A_0	A_2/A_0	<i>Type</i>
12.10202.285	2.511844	3.118910	—	0.8054	0.260	—	RR12
12.10443.367	2.971251	3.701164	—	0.8028	0.294	—	RR12
9.4278.179	3.059812	3.801934	—	0.8048	0.296	—	RR12
2.5023.5787	3.081326	3.068358	3.073338	1.0042	1.000	0.926	RR1- ν 2
11.8987.787	3.288101	3.238294	3.129587	1.0154	0.638	0.345	RR1- ν 2
15.9947.338	3.469549	3.421443	3.434602	1.0141	0.559	0.419	RR1- ν 2